AN X-RAY DIFFRACTION STUDY OF

$(NH_4)_2TeBr_6$ AND Cs_2TeBr_6

By

AJIT KUMAR DAS, M.Sc.

A Thesis

Submitted to the Faculty of Graduate Studies

in Partial Fulfilment of the Requirements

for the Degree

Master of Science

McMaster University

May, 1967

MASTER OF SCIENCE (1967)
(Physics)

McMaster University
Hamilton, Ontario

TITLE: An X-ray Diffraction Study of $(NH_4)_2TeBr_6$ and Cs_2TeBr_6

AUTHOR: Ajit Kumar Das, M.Sc. (Bihar University, India)

SUPERVISOR: Dr. I. D. Brown

NUMBER OF PAGES: (vi), 77

SCOPE AND CONTENTS:

The crystal structures of $(NH_4)_2TeBr_6$ and Cs_2TeBr_6 have been reinvestigated using X-ray diffraction from powders and single crystals. Three dimensional single crystal intensity data obtained photographically have been used to refine these structures, which are of the cubic K_2PtCl_6 type, by a full matrix least squares analysis. The Te-Br bond is found to be 2.70Å in both crystals after correction for the thermal motion of the atoms.

A phase transition in $(NH_4)_2TeBr_6$ has been observed at about 183°K. From an examination of Weissenberg photographs taken at 163°K, the low temperature phase is found to be tetragonal, space group $P4/_mnc$ (D_{4h}^6) with $\underline{a}$ = 7.501±0.005Å and $\underline{c}$ = 10.765±0.005Å. The transformation in this case is probably similar to that reported in other isomorphous crystals, e.g., K_2SnBr_6.

A review of other crystals with similar structure is included in this thesis and the theory of X-ray diffraction as applicable to the present problem is discussed briefly.

ACKNOWLEDGEMENTS

"One must learn by doing the thing; for though you think you know it, you have no certainty until you try."

SOPHOCLES

I should like to express my sincere gratitude to Dr. I. D. Brown for his encouragement and guidance in this research.

Thanks are due to Dr. C. Calvo for some helpful discussions and to Messrs. J. K. Brandon and B. E. Robertson for suggestions and assistance at various stages of this work.

Thanks are also due to the National Research Council of Canada for supporting this work, and to the McMaster University for a graduate scholarship.

TABLE OF CONTENTS

		PAGE
CHAPTER 1:	INTRODUCTION	1
CHAPTER 2:	THEORY OF STRUCTURE DETERMINATION	9
2.1	Theory of X-ray Diffraction by a Crystal Lattice	9
2.2	Measurement of Lattice Constants	13
2.3	Measurement of Intensities	15
2.4	Structure Factor Calculation	19
2.4A	Temperature factor	20
2.5	Refinement	21
2.5A	The Method of Least Squares	21
CHAPTER 3:	PREPARATION OF COMPOUNDS AND THEIR LATTICE CONSTANTS	24
3.1	Preparation of Compounds	24
3.2	Determination of Accurate Cell Constants	25
CHAPTER 4:	MEASUREMENT OF INTENSITIES	35
4.1	Size and Shape of Crystal	35
4.2	Measurement of Intensities	38
4.3	Intensity Corrections and Relative Scaling of Layers	39
CHAPTER 5:	STRUCTURE ANALYSIS AND REFINEMENT	41
5.1	Structure Factor Calculation	41
5.2	Refinement	45
CHAPTER 6:	DESCRIPTION OF THE STRUCTURES	52
CHAPTER 7:	PHASE TRANSITION IN $(NH_4)_2TeBr_6$	58
7.1	Introduction	58
7.2	Low Temperature Polarizing Microscope	60
7.3	Measurement of Transition Temperature	63
7.4	Weissenberg Photographs and their Interpretation	64
BIBLIOGRAPHY		75

LIST OF ILLUSTRATIONS

FIGURE		PAGE
1	The unit cell of Potassium hexachloroplatinate, K_2PtCl_6	2
2a	Scattering of X-rays by scatterers situated at two lattice points	10
2b	Relationship between the vectors $\underline{s}$, $\underline{s_o}$ and $\underline{S}$	10
3	A schematic view of the powder method	14
4	The Straumanis method of film mounting	26
5	Sections through the cation perpendicular to (111) direction in (a) Cs_2TeBr_6 and (b) $(NH_4)_2TeBr_6$	56
6	A schematic view of the low temperature polarizing microscope	61
7	Compound Weissenberg photographs of $(NH_4)_2TeBr_6$ taken at 163°K and 298°K about (a) $(1\bar{1}0)$ as rotation axis and (b) (100) as rotation axis	65
8a	Transformation of the C-face centered tetragonal cell to a primitive cell	68
8b	Reciprocal lattice: C-face centered and primitive tetragonal cell indexings	68
9	Twinning in $(NH_4)_2TeBr_6$: Composite reciprocal lattice perpendicular to the C-centered pseudo-cubic tetragonal (a) $[1\bar{1}0]$ and $[0\bar{1}1]$ directions, and (b) [100] and [001] directions	70

LIST OF TABLES

TABLE		PAGE
I	Structures of some $A_2^{I}M^{IV}X_6$ type crystals	6
II	The observed and calculated d-spacings for $(NH_4)_2TeBr_6$	30
III	The observed and calculated d-spacings for Cs_2TeBr_6	31
IVA	Accurate lattice constant of $(NH_4)_2TeBr_6$	32
IVB	Accurate lattice constant of Cs_2TeBr_6	33
V	Crystal data for $(NH_4)_2TeBr_6$ and Cs_2TeBr_6	34
VI	Atomic parameters derived from the final least squares refinement	49
VII	The observed and calculated structure factors for $(NH_4)_2TeBr_6$	50
VIII	The observed and calculated structure factors for Cs_2TeBr_6	51
IX	Interatomic distances and thermal motions in M_2TeBr_6 crystals	57
X	The unit cells and space groups of $(NH_4)_2TeBr_6$ and K_2SnBr_6 crystals	74

CHAPTER I

INTRODUCTION

The crystal structures of a large number of compounds of the general formula $A_2^{I}M^{IV}X_6$ (where A^{I} = K, NH_4, Rb or Cs; M^{IV} = Pt, Sn, Se, Te, Re etc., and X = Cℓ, Br or I) have been determined by several workers (e.g. Ewing and Pauling, 1928; Engel, 1935; Hoard and Dickinson, 1933; Sieg, 1932; Bagnall et al., 1955, Templeton and Dauben, 1951) using X-ray diffraction. Most of the early investigations involved the measurement of only the powder photographs of these compounds and do not give accurate positional and thermal parameters of the atoms. The great majority of these compounds crystallize in the cubic potassium hexachloroplatinate ($K_2PtC\ell_6$) structure (Ewing and Pauling, 1928), space group $Fm\bar{3}m(O_h^5)$. In the $K_2PtC\ell_6$ structure (Fig. 1), which is basically an anti-fluorite structure, the regular octahedral anions ($PtC\ell_6^{2-}$) are arranged on a face centered cubic lattice while each cation (K^+) occupies the tetrahedral hole formed by four neighbouring anions. The Pt-Cℓ bonds lie along the principal axes of the cubic unit cell. Each K^+ ion in this structure is surrounded by twelve chlorine atoms at the same distance from it.

However, while most of these compounds have the $K_2PtC\ell_6$ structure, a few of them have been reported to possess distorted forms of this structure. Such distortions have been found at room temperature in K_2SnBr_6 (Markstein and Nowotny, 1938) and K_2TeBr_6 (Brown, 1964). The former crystal has a tetragonal structure while the latter is monoclinic.

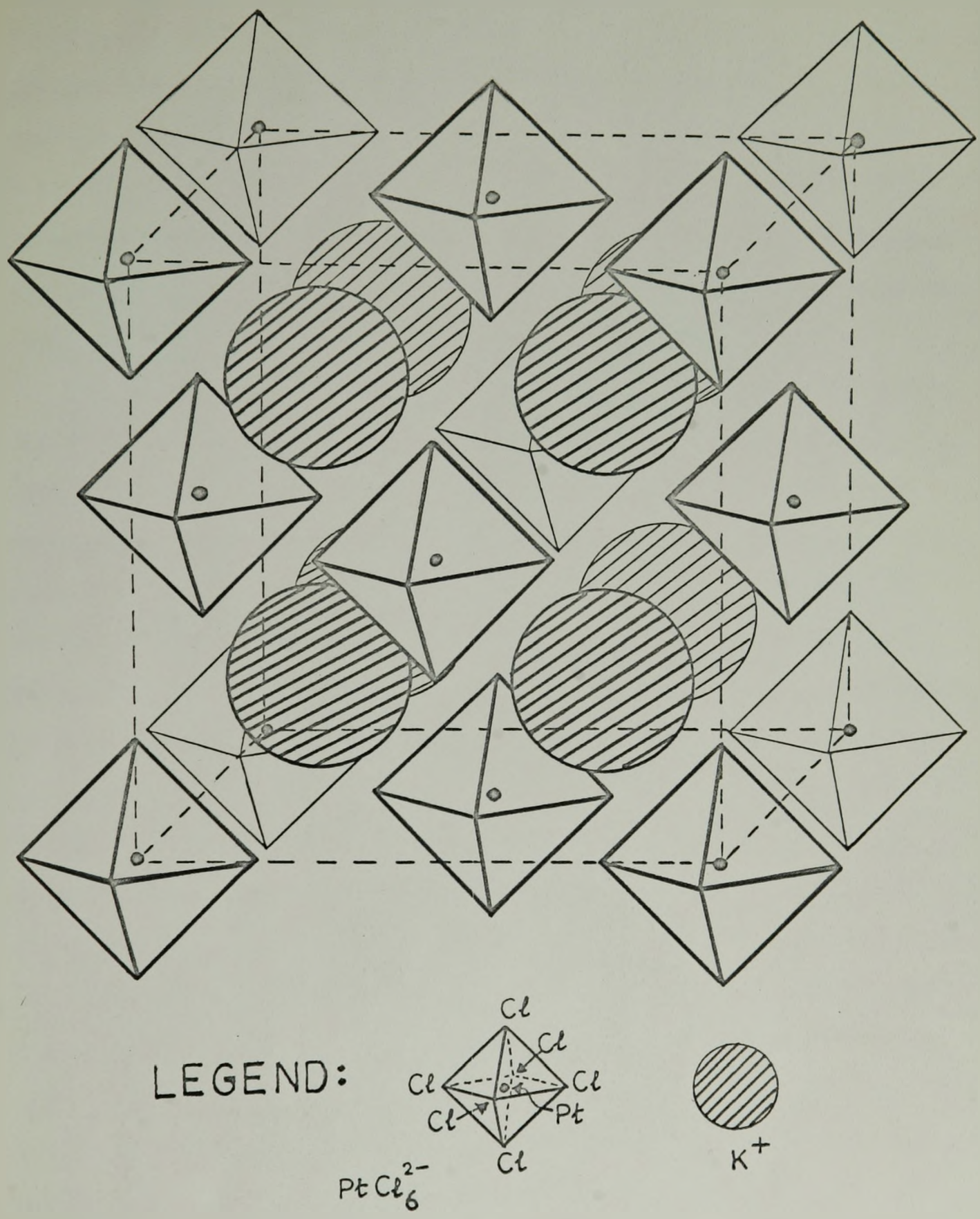

Fig. 1 The unit cell of Potassium hexachloroplatinate, K_2PtCl_6

Similar distortions have also been noted in many compounds from nuclear quadrupole resonance (NQR) measurements, and the existence of specific heat anomalies in others suggests that these structures are also distorted. Nakamura and his co-workers (1960, 1962 a, b; 1963, 1964) have used the quadrupole resonance of halogens to examine the hexahalogenate anions of a variety of metals* including Pt(IV), Sn(IV), Te(IV), Se(IV) and Re(IV). In many cases they have found phases where the resonance signals are split, indicating the presence of non-equivalent halogen atoms in these structures. Such structures must therefore have symmetries lower than cubic.

Further, from the measurement of the heat capacities of $(NH_4)_2SnCl_6$ and $(NH_4)_2SnBr_6$ at low temperatures, Morfee et al. (1960) have suggested that some distortions might occur in these compounds, both of which have the K_2PtCl_6 structure at room temperature, but exhibit specific heat anomalies between 100°K and 300°K. The anomaly in $(NH_4)_2SnCl_6$ is small and occurs between 235° and 245°K, and it is unlikely that a change in the crystal structure is involved. But in $(NH_4)_2SnBr_6$, the specific heat anomaly is large and it is quite possible that a change in the structure may occur at low temperature. Busey et al. (1962) has observed the specific heat anomalies in K_2ReCl_6 at 76°, 103° and 111°K which, they suggest, are due to some distortions in the crystal structure of the compound. Furthermore, recent neutron diffraction measurements on K_2ReCl_6 by Smith and Bacon (1963) confirm a change in the symmetry from the space group Fm3m at room temperature to a space group of lower symmetry (Pn3 or Pn3m), although still cubic, below 77°K. Similar specific heat anomalies have been reported recently by Busey and his co-workers (1965) in K_2ReBr_6 at 225° and 245°K. This compound, which possesses the K_2PtCl_6 structure at room temperature (Templeton and Dauben, 1951), has been found from NQR measurements to undergo three close

---

*See also Ito et al. (1961,1963) for similar works on compounds of Pd(IV), Ir(IV) and Os(IV).

transitions below 270°K (Ikeda et al., 1963; 1965).

An explanation for these distortions has been proposed by Brown (1964), who suggests that if the c tion is very much smaller than the cavity into which it fits, the anions will reorient themselves in a way so as to reduce the effective cavity size and thus lock the cation in place. A similar idea has also been suggested by Morfee et al. (1960) to explain the specific heat anomaly in $(NH_4)_2SnBr_6$ at low temperature. Further, Brown (1964) has proposed a criterion to decide whether any given structure is expected to be distorted from the K_2PtCl_6 type. This criterion is based on the radius ratio, defined as the ratio of the cation radius to the radius of the cavity formed by the twelve halogen atoms which surround it. He has noted that:

(1) crystals with a radius ratio of less than about 0.89 are distorted from the cubic structure at room temperature;

(2) crystals with a radius ratio between about 0.89 and 0.98 are cubic at room temperature but distort at lower temperature; and

(3) crystals with a radius ratio greater than 0.98 are not distorted from the cubic structure at any temperature.

The structures of some A_2MX_6 crystals arranged in order of radius ratio are listed in Table I.

The work described in this thesis deals with the studies of the crystal structures of $(NH_4)_2TeBr_6$ and Cs_2TeBr_6 at room temperature and an examination of the first phase transition in $(NH_4)_2TeBr_6$ below room temperature. This work was undertaken to examine the influence of the cation on the bonding within the $TeBr_6^{2-}$ ion and to study the nature of distortion in $(NH_4)_2TeBr_6$

crystal below the transition temperature of 221°K reported by Nakamura and his co-workers (1962a). Although both $(NH_4)_2TeBr_6$ and Cs_2TeBr_6 were known to possess the cubic K_2PtCl_6 structure at room temperature (Hanojlović, 1957; Swanson et al., 1957, 1960; Bagnall et al., 1955), it was necessary to obtain more accurate information about their room temperature structures for the present investigation. In the present study, the accurate cell constants of both crystals have been determined from their powder photographs and the single crystal intensity data have been used to determine accurate positional and thermal parameters of atoms in each crystal. The first transition temperature in $(NH_4)_2TeBr_6$ has been redetermined and the space group and lattice parameters of the low temperature phase are reported.

TABLE I

Structures of some $A_2^{I}M^{IV}X_6$ type crystals

Compound	Radius[a] ratio	Structure[b]	Method[c] X-ray	NQR	Specific heat
(1) Crystals which are distorted from cubic at room temperature:					
K_2TeBr_6	0.83	Monoclinic at 293°K	1	2	
K_2SnBr_6	0.86	Tetragonal at 293°K, Cubic above 400°K	3,4	5	6
Rb_2TeI_6	0.86	Tetragonal at 293°K, Cubic above 328°K		7	
K_2TeCl_6	0.89	Monoclinic at 293°K	8	2	
K_2PbCl_6	0.91	Monoclinic at 300°K, Cubic above 333°K	9		
(2) Crystals which are cubic at room temperature but distorted at low temperature:					
Rb_2SnI_6	0.88	Cubic at 293°K	10		
$(NH_4)_2TeBr_6$	0.90	Cubic above 168°K	11,12	2	
K_2ReBr_6	0.91	Cubic above 245°K	13,14	15,16	17
K_2SnCl_6	0.92	Cubic above 262°K	8		6
K_2SeBr_6	0.93	Cubic above 240°K	18	19	
$(NH_4)_2SnBr_6$	0.93	Cubic at 293°K	3	5	6
$(NH_4)_2TeCl_6$	0.96	Cubic above 77°K	20	2	
K_2ReCl_6	0.97	Cubic above 111°K	14,21,22	15,16	23
(3) Crystals which are cubic at all temperatures:					
K_2PtCl_6	0.98	cubic	24	25	
Cs_2TeI_6	1.00	cubic	26	2	
Cs_2TeBr_6	1.07	cubic	12,27	2	

(continued)

[a] For definition of the radius ratio, see ref. 1.

[b] 'Cubic' in this column and at other places in the table means the K_2PtCl_6 structure.

[c] The numbers in different columns indicate the respective references as mentioned below:

1. Brown (1964)
2. Nakamura et al. (1962a)
3. Markstein and Nowotny (1938)
4. Galloni et al. (1962)
5. Nakamura et al. (1962b)
6. Morfee et al. (1960)
7. Nakamura and Kubo (1964)
8. G. Engel (1935)
9. Brown and Lim (1966)
10. Werker (1939)
11. Manojlović (1957)
12. Present work
13. Templeton and Dauben (1951)
14. Schwochau (1964)
15. Ikeda et al. (1963)
16. Ikeda et al. (1965)
17. Busey et al. (1965)
18. Hoard and Dickinson (1933)
19. Nakamura et al. (1963)
20. Hazell (1966)
21. Aminoff (1936)

22. Smith and Bacon (1963), (neutron diffraction measurement)

23. Busey et al. (1962)

24. Ewing and Pauling (1928)

25. Nakamura et al. (1960)

26. Manojlović (1956)

27. Bagnall et al. (1955)

CHAPTER 2

THEORY OF STRUCTURE DETERMINATION

In this chapter a brief discussion of the theory of structure determination is given to provide a background to the present investigation.

2.1 Theory of X-ray Diffraction by a Crystal Lattice:

A crystal consists of a three dimensional array of identical groups of atoms. Alternatively, a crystal can be considered as made up of identical space filling blocks, called the unit cells, which are repeated through the whole body of the crystal and related to each other by translational symmetry. This network of unit cells constitute the direct or crystal lattice. Such an array of cells containing atoms, when exposed to a beam of X-rays, gives rise to a diffraction pattern in which the positions of the peaks depend on dimensions of the unit cell and the intensities of the peaks depend on the distribution of electrons (and hence atoms) within the cell.

Consider a parallel beam of X-rays propagating in the direction $\underline{s}_o$. Let the rays be incident on two scatterers situated at lattice points P_1 and P_2 (see Fig. 2a), and separated by a distance $\underline{r}$. Consider that the rays are diffracted along the direction $\underline{s}$. Also let $|\underline{s}_o| = |\underline{s}| = 1/\lambda$, where λ is the wavelength of the radiation. Now to find the resultant diffraction effect we consider the path difference between these rays. From Fig. 2a the path difference is given by

$$P_1N - MP_2 = \lambda(\underline{r} \cdot \underline{s} - \underline{r} \cdot \underline{s}_o) \qquad (2.1)$$

$$= \lambda \underline{r} \cdot (\underline{s} - \underline{s}_o) \qquad (2.2)$$

$$= \lambda \underline{r} \cdot \underline{S}$$

where $\underline{S} = \underline{s} - \underline{s}_o$. (See Fig. 2b)

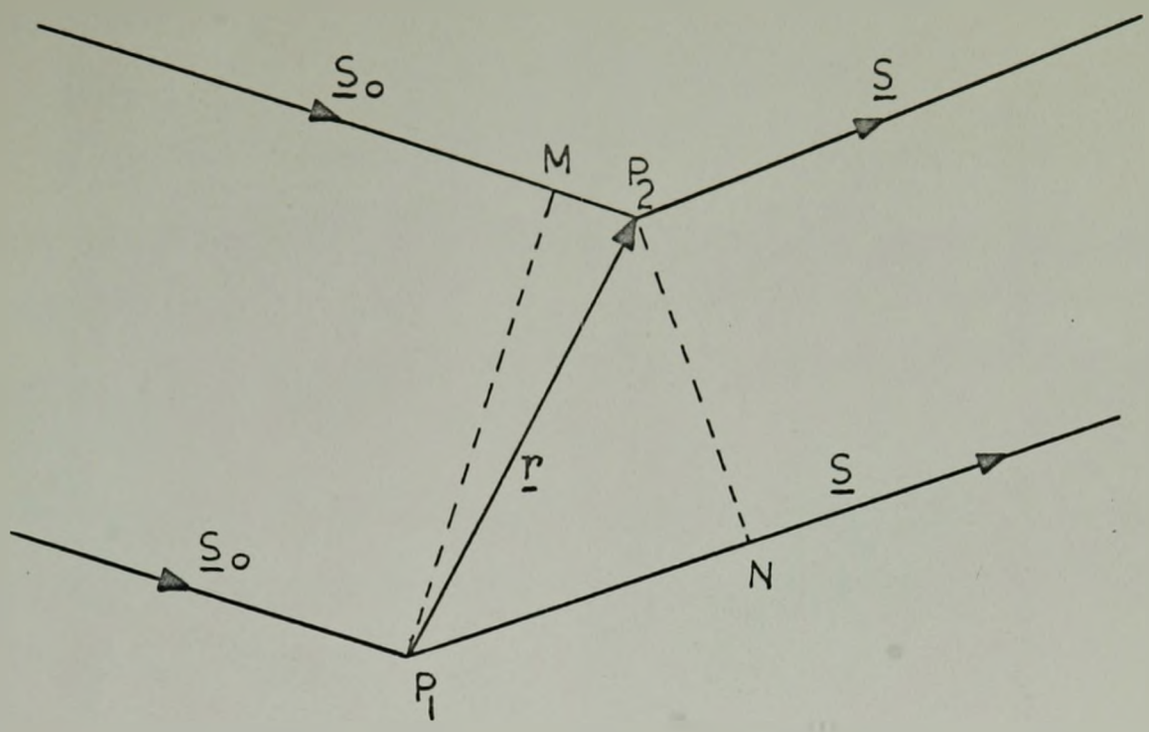

Fig. 2a Scattering of X-rays by scatterers situated at two lattice points

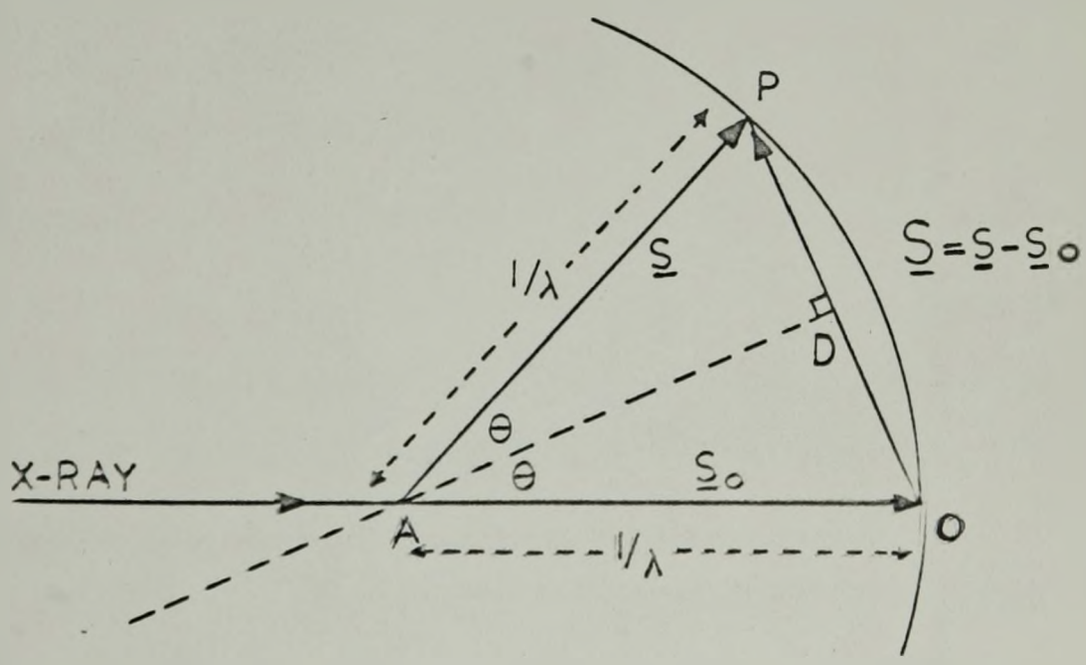

Fig. 2b Relationship between the vectors $\underline{s}$, $\underline{s}_o$ and $\underline{S}$.

Hence for a diffraction maximum,

$$\lambda\, \underline{r} \cdot \underline{S} = n\lambda$$

$$\text{or,} \quad \underline{r} \cdot \underline{S} = n \tag{2.3}$$

where n is an integer. Let the angle between $\underline{s_o}$ and $\underline{s}$ be 2θ. Then from Fig. 2b we find that

$$|\underline{S}| = |\underline{s} - \underline{s_o}| = \frac{2\sin\theta}{\lambda} \quad . \tag{2.4}$$

Suppose that the primitive translations of the lattice are denoted by $\underline{a}$, $\underline{b}$ and $\underline{c}$. Since we have considered the scatterers located at lattice points P_1 and P_2, the vector $\underline{r}$ can be specified as

$$\underline{r} = m_1\underline{a} + m_2\underline{b} + m_3\underline{c} \tag{2.5}$$

where m_1, m_2 and m_3 are integers. Thus from the relation (2.3),

$$\underline{r} \cdot \underline{S} = m_1\underline{a} \cdot \underline{S} + m_2\underline{b} \cdot \underline{S} + m_3\underline{c} \cdot \underline{S} = n \tag{2.6}$$

Since m_1, m_2 and m_3 are independent, each term in (2.6) must be equal to an integer. That is,

$$\begin{aligned} \underline{S} \cdot \underline{a} &= h \\ \underline{S} \cdot \underline{b} &= k \\ \underline{S} \cdot \underline{c} &= \ell \end{aligned} \tag{2.7}$$

where h,k and ℓ are integers. These equations are known as the Laue equations and they must be simultaneously satisfied by a diffracted beam in order that it may have maximum intensity.

Again, from Fig. 2b it is apparent that the vector $\underline{S}$ lies along the direction perpendicular to the bisector of the angle between the incident and the diffracted rays. Hence $\underline{S}$ maybe identified as normal to the plane AD which makes equal angles with the incident and diffracted beam and it can be

shown (Lipson and Cochran, 1953, p.5) that for the diffraction maximum to occur, $\underline{S}$ is normal to a lattice plane with Miller indices h,k and ℓ.

Now, let the vector $\underline{S}$ be expressed by

$$\underline{S} = n_1\underline{a}^* + n_2\underline{b}^* + n_3\underline{c}^* \qquad (2.8)$$

where $\underline{a}^*$,$\underline{b}^*$, and $\underline{c}^*$ denote three non-coplanar vectors in the reciprocal space, and n_1,n_2 and n_3 are coordinates. For a diffraction maximum, the vector $\underline{S}$ must satisfy the Laue conditions (2.7). If a^*,b^* and c^* are chosen so that

$$\underline{a}^* \cdot \underline{a} = \underline{b}^* \cdot \underline{b} = \underline{c}^* \cdot \underline{c} = 1$$

and (2.8a)

$$\underline{a}^* \cdot \underline{b} = \underline{b}^* \cdot \underline{a} = \underline{a}^* \cdot \underline{c} = \underline{c}^* \cdot \underline{a} = \underline{b}^* \cdot \underline{c} = \underline{c}^* \cdot \underline{b} = 0$$

then, n_1=h, n_2=k and n_3=ℓ represents the Laue conditions. Thus the values of $\underline{S}$ corresponding to diffraction maxima are given by

$$\underline{S} = h\underline{a}^* + k\underline{b}^* + \ell\underline{c}^* \qquad (2.9)$$

That is the diffraction maxima are observed only for those values of $\underline{S}$ which lie on a lattice formed by the unit vectors $\underline{a}^*$,$\underline{b}^*$ and $\underline{c}^*$ — the reciprocal lattice.

The Laue equations can also be expressed in the form:

$$\begin{aligned} (\underline{a}/h) \cdot \underline{S} &= 1 \\ (\underline{b}/k) \cdot \underline{S} &= 1 \\ (\underline{c}/\ell) \cdot \underline{S} &= 1 \end{aligned} \qquad (2.10)$$

The projection of either of the vectors $\underline{a}$/h, $\underline{b}$/k and $\underline{c}/\ell$ on $\underline{S}$ is equal to the perpendicular distance of the plane hk from the origin - which, in general, is the lattice spacing, d, of the set of planes (hkℓ).

Thus,

$$d = (\underline{a}/h) \cdot \frac{\underline{S}}{|\underline{S}|}$$

and using the first Laue condition (2.10)

$$d = \frac{1}{|\underline{S}|} \tag{2.11}$$

Since $|\underline{S}| = \frac{2\sin\theta}{\lambda}$ (see Eqn. (2.4)), we get from (2.11)

$$2d_{hk\ell} \sin\theta = \lambda \tag{2.12}$$

This is the well-known Bragg equation. The quantity n(called the order of reflection) which usually appears in Bragg equation is here included in spacing d_H ($H = h,k,\ell$) since the interplanar spacing corresponding to indices nH is regarded as $\frac{1}{n}$th. of the spacing corresponding to indices H.

Thus the conditions for the diffraction of X-rays from a set of crystal planes are the following:

(a) The angle of incidence is equal to the angle of diffraction (θ) both being measured by the angles that the incident and diffracted rays make with the ($hk\ell$) crystal plane.

(b) The incident ray, the diffracted ray and the normal to the crystal plane are coplanar.

(c) The Bragg equation (2.12) must be satisfied.

2.2 Measurement of Lattice Constants:

In principle, both powder and single crystal diffraction can be used to determine the lattice parameters of any crystal. For cubic, tetragonal and hexagonal crystals, accurate cell parameters can be obtained relatively easily from their powder diagrams. In fact, the powder diagrams are sometimes sufficient for complete analysis of simple structures.

In the powder method developed by Debye and Scherrer, a monochromatic beam of X-rays is allowed to fall on the specimen in powdered form. Since the crystallites are oriented randomly in the sample, it is quite probable that some of them are in a position to reflect the incident beam in such a way as to satisfy the Bragg condition (eqn. 2.12):

$$2d_{nk\ell} \sin\theta = \lambda$$

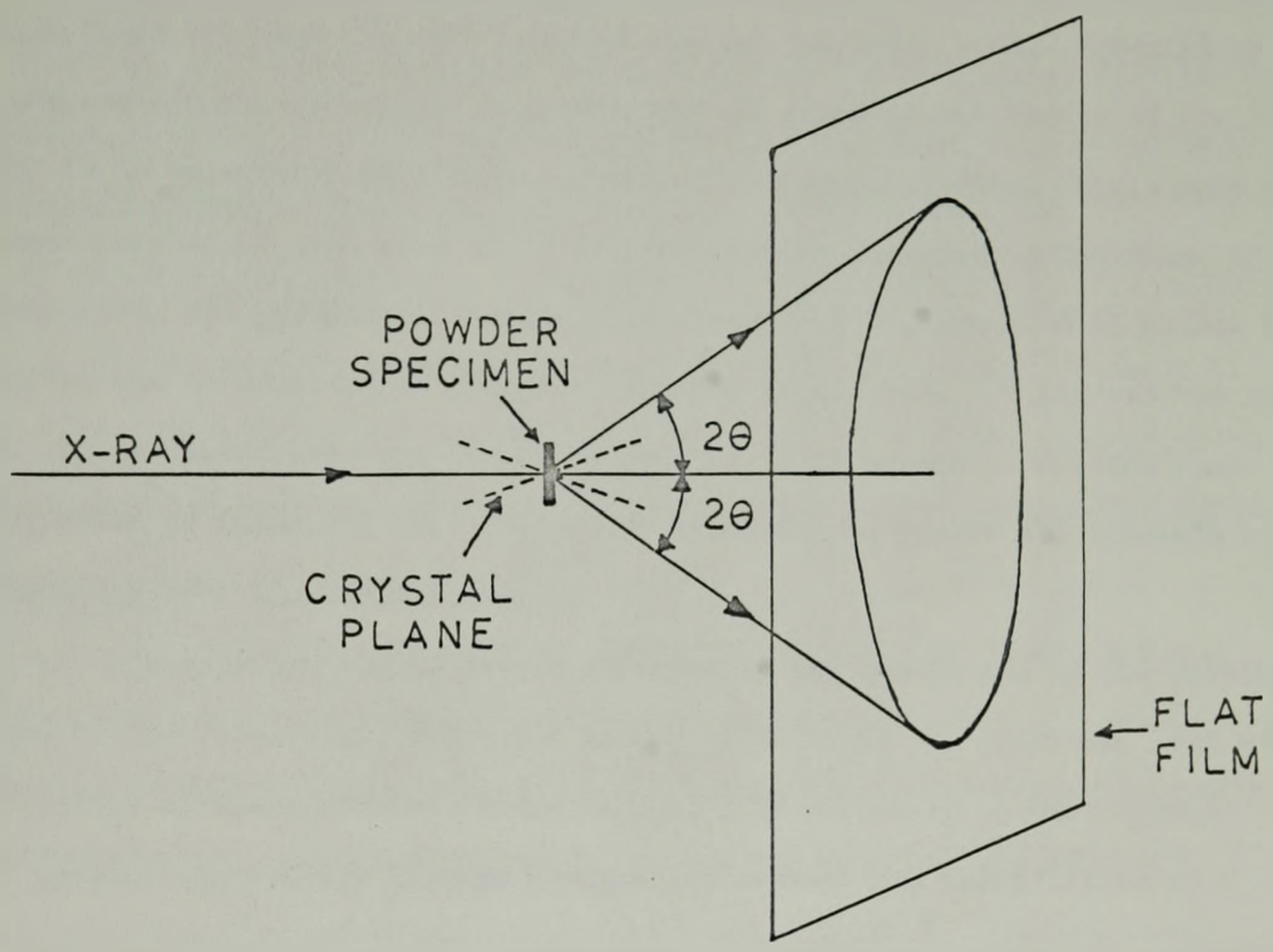

Fig. 3 A schematic view of the powder method

The diffracted rays lie on the surface of a cone centered on the direction of the incident beam with the semi-vertical angle 2θ, where θ is the corresponding Bragg angle (Fig. 3).

In practice, a flat film is rarely used to obtain the powder diagrams. The normal Debye-Scherrer camera consists of a cylindrical metal enclosure with holes provided for entrance and exit of the X-ray beam. A capillary tube containing the sample in powder form is fixed at the centre of the camera, and it is surrounded by a narrow strip of photographic film. While only a small portion of each cone of diffracted rays is recorded on the film, in principle, all possible reflections corresponding to high as well as low Bragg angles can be recorded if suitable exposure is allowed. To improve the quality of the powder diagram the sample is rotated so as to ensure unifrom distribution of intensity over the powder lines and to record all possible reflections from the crystal planes.

Various systematic errors inherent in the camera and in the development of the film (e.g., those due to eccentricity of the specimen, lack of knowledge of the effective camera radius, film shrinkage in development) can be reduced appreciably if high Bragg angle reflections (also called back reflections) are used in the calculation of the lattice parameters (Buerger, 1942; Ch. 20).

2.3 Measurement of Intensities:

The intensities of reflections are used to determine the positions of atoms within the unit cell. The structure factor, $F(\underline{H})$, of a reflection $\underline{H}(=h,k,\ell)$ is given by the Fourier transform of the electron density, $\rho(xyz)$ within the cell (Lipson and Cochran, 1953, p.11) as:

$$F(H) = V \int_{x=0}^{1}\int_{y}\int_{z} \rho(xyz) \exp 2\pi i(hx + ky + \ell z)\, dxdydz \qquad (2.13)$$

where V denotes the volume of the unit cell, and x,y and z are the fractional coordinates of the volume element (Vdxdydz) considered.

$F(\underline{H})$ (see section 2.4 for further details) in Eq.(2.13) is a complex quantity, representing not only the amplitude but also the phase of the diffracted beam, and it is related to the observed intensity, I, of the diffracted beam by the expression:

$$I(H) \propto F(\underline{H}) \cdot F^{*}(\underline{H}) = \left|F(\underline{H})\right|^{2} \qquad (2.14)$$

Thus from the measurement of intensities, the moduli of the structure factors can be evaluated and these can then be used in the determination of the crystal structure (Buerger, 1960; Ch.22), provided a trial model of the structure is known.

The diffraction pattern is frequently recorded on films on which the diffraction maxima appear as spots of varying intensity. However, the measurement of these intensities is encompassed with several difficulties, for example, how should corrections be made for variation in shape and size of the spots, non-uniform distribution of intensity over the spots, and the presence of different background around the spots located in different areas on the film. In a real crystal, due to imperfection, adjacent volume units are not exactly parallel and so the crystal must be turned slightly to bring each such volume unit into the perfect Bragg condition for a reflection to occur. This causes the reflection spots to be drawn out over a small range. The degree of imperfection may vary with direction in the crystal and differs for different reflections.

Thus the peak intensity of a reflection does not necessarily give a reliable measure of the structure amplitude, $|F(\underline{H})|$. A better measure of the reflecting power can be obtained by summing the energy reflected by the set of crystal planes as the crystal is rotated through the angles close to the ideal Bragg angle, that is, by integrating the intensities as the crystal is uniformly rotated through the region of a Bragg reflection.

An expression for the integrated intensity has been deduced by James (1962; p.41). For reflection from a crystal element of volume ΔV in which the absorption of X-rays maybe neglected, the integrated intensity is given by:

$$\frac{E\omega}{I_o} = \int_{\theta_o-\epsilon}^{\theta_o+\epsilon} R(\theta)d\theta = Q\ \Delta V \qquad (2.15)$$

where I_o is the energy incident per unit area per unit time on the crystal and E is the energy reflected (or diffracted) by the crystal when it rotates with uniform angular velocity ω about an axis parallel to the set of crystal planes which reflect the incident beam at the Bragg angle θ_o. Here ϵ denotes a small deviation from the ideal Bragg position which includes the contribution of all the reflected radiation. $R(\theta)$ is the reflecting power (at an angle θ) of the crystal element per unit incident intensity, I_o. The quantity Q can be expressed as

$$Q = \left(\frac{e^2}{mc^2}\right)^2 N^2\lambda^3 \quad |F(\underline{H})|^2 \ \frac{(1+\cos^2 2\theta)}{2\sin 2\theta} \qquad (2.16)$$

where N is the number of unit cells per unit volume of the crystal, and $F(\underline{H})$ is the structure factor (see eqn. (2.13)).

The factor $\frac{1+\cos^2 2\theta}{2}$ in Eqn. (2.16) is called the polarization factor (p) and is the amount by which the intensity of the diffracted beam

is diminished due to partial polarization on diffraction. The factor, $\frac{1}{\sin 2\theta}$ known as the Lorentz factor (L), is proportional to the time that the crystal takes to pass through a reflecting position. In general, this factor varies not only with the Bragg angle but also with the particular arrangement by which the diffraction pattern is recorded. Usually the correction for the Lorentz and polarization effects is applied in the combined form as $(Lp)^{-1}$. The observed structure amplitude $\left|F(\underline{H})\right|$ of a reflection can be evaluated from its measured intensity (I) using the relation:

$$\left|F(\underline{H})\right| = K\left(\frac{I}{Lp}\right)^{\frac{1}{2}} \qquad (2.17)$$

where K is a proportionality constant dependent on the wavelength and crystal-size.

The visual estimation of intensities on photographic films is carried out by comparing the reflection spot with one of a series of spots prepared by photographing one particular reflection at different known exposure times. The peak intensity of a reflection is measured by this method and in the visual estimation of intensities it is commonly assumed that the peak intensity is proportional to the integrated intensity. In fact, this is frequently not so due to non-uniformity in size of the spots.

To integrate the intensities, the cross sections of the reflections should be taken into account, since the integration calls for summing the intensity from all parts of the spot. This is achieved by recording the reflection on a film which is moved over a series of regular small intervals so that the density of blackening at the centre of the spot on the film attains a constant value which measures the integrated intensity of the reflection (Buerger, 1960; p.103).

A mechanical device for recording the integrated intensities of the

reflections on the Weissenberg film has been described by Wiebenga and Smits (1950), and on the Buerger precession camera by Nordman et al. (1955). A microdensitometer can be used to measure the integrated intensities of the reflections. The densitometer traces of the spots will show plateau like profiles whose heights (corrected for the background) are proportional to the integrated intensities.

2.4 Structure Factor Calculation:

The structure factor $F(\underline{H})$ of reflection $\underline{H}$(Lipson and Cochran, 1953; p.10) is given by eqn. (2.13) and can also be expressed in the form:

$$F(\underline{H}) = \sum_{j=1}^{n} f_j \exp 2\pi i(hx_j + ky_j + \ell z_j) \qquad (2.18)$$

where the summation extends over all atoms in the unit cell. x_j, y_j and z_j denote the fractional coordinates of the jth atom in the unit cell. The atomic scattering factor f_j is the scattering power of the jth atom and is equal to the Fourier transform of the electron density of the atom. Since the charge distribution in an atom is assumed to have spherical symmetry, the atomic scattering factor f_j depends only on the angle of diffraction and the wavelength λ of the incident radiation. The scattering power of an atom is thus a function of $(\frac{\sin\theta}{\lambda})$ and it decreases as θ increases due to the interference of the scattered waves from different parts of the atom. For $\theta = o$, f_j is proportional to the number of electrons Z (atomic number) of the atom. In general, the structure factor $F(\underline{H})$ is a complex quantity and can be expressed as

$$F(\underline{H}) = A(\underline{H}) + i\,B(\underline{H}) \qquad (2.19)$$

where

$$A(H) = \sum_{j}^{n} f_j \cos 2\pi(hx_j + ky_j + \ell z_j)$$

$$B(H) = \sum_{j}^{n} f_j \sin 2\pi(hx_j + ky_j + \ell z_j) \qquad (2.20)$$

In a centro symmetric structure, for each atom at the point (x,y,z) in the unit cell there is an equivalent atom at $(\bar{x},\bar{y},\bar{z})$. The contribution of this pair (and all pairs in the unit cell) to the structure factor is given by

$$f\left[\cos 2\pi(hx + ky + \ell z) + i \sin 2\pi(hx + ky + \ell z) + \cos 2\pi(hx + ky + \ell z) - i \sin 2\pi(hx + ky + \ell z)\right]$$

$$= 2f \cos 2\pi(hx + ky + \ell z)$$

Hence,

$$F(\underline{H}) = 2 \sum_{j=1}^{n/2} f_j \cos 2\pi(hx_j + ky_j + \ell z_j) \qquad (2.21)$$

where the summation now is over half the atoms in the unit cell. Thus for a centro symmetric structure

$$F(\underline{H}) = A(\underline{H}) \quad \text{and} \quad B(\underline{H}) = 0 \qquad (2.22)$$

2.4A Temperature Factor:

In a crystal at any temperature the atoms are undergoing thermal vibrations. It is assumed that the atoms can be treated as uncoupled harmonic oscillators and their vibrations, in general, are anisotropic and of different amplitudes. The effective scattering factor of the jth atom thus is given by

$$f_j = f_j^o \exp\left[-(\beta_{11}h^2+\beta_{22}k^2+\beta_{33}\ell^2+2\beta_{12}hk+2\beta_{23}k\ell+2\beta_{13}h\ell)\right] \qquad (2.23)$$

where f_j^o is the scattering factor of the jth atom being at rest, and the β's are the coefficients of the anisotropic temperature factor.

When the thermal motion of the jth atom is isotropic in nature, its effective scattering factor is given by

$$f_j = f_j^o \exp(-B_j S^2) \qquad (2.24)$$

where $S = \sin\theta/\lambda$ and B_j is a constant.

2.5 Refinement:

The magnitudes of the structure amplitudes, $|F(\underline{H})|$, are derived from observations of intensities. But the Fourier transform of these amplitudes (Lipson and Cochran, 1953, Ch. 7) which gives a direct image of the electron density, can be carried out only if the relative phases of the structure factors, $F(\underline{H})$, are also known. Usually the phases are assumed to be the same as those calculated from a trial structure.

In the present investigation a trial structure was available from the previous works (see text, Ch. 1), but could have been derived from the solution of a Patterson function (Lipson and Cochran, 1953; Ch. 6). With modern computing facilities the crystal structure can be refined by the method of Least Squares (see section 2.5A). By this method it is possible to refine simultaneously all the parameters of atoms in the asymmetric unit using three dimensional intensity data.

2.5A The Method of Least Squares:

The method of least squares can be used to refine crystal structures by minimizing a suitable function of the measured structure amplitudes (F_H^o) and those (F_H^c) calculated from the trial structure with respect to the structure parameters (P_i). Since it is assumed that the errors in F_o's follow the normal or Gaussian distribution, the best atomic parameters are those which result in minimization of the sum of weighted squares of the

residual, R.

$$R = \sum_{H} w_H \left(|F_H^o| - |F_H^c (P_i)| \right)^2 \qquad (2.25)$$

where w_H is the weight of the Hth reflection and is proportional to the inverse of the square of the standard error of F_H^o. The parameters (P_i) include positional coordinates, isotropic or anisotropic temperature factors of the atoms and the scale constants to be applied to the observed structure factors.

The quantities to be determined are the corrections p_i to the trial parameters p_i such that the new set F parameters $P_i (= p_i + \Delta p_i)$ minimizes R (see equation (2.25)). We can express $F_H^c(p_i + \Delta p_i)$ by the Taylor Series expansion as

$$F_H^c(P_i) = F_H^c(p_i + \Delta p_i) = F_H^c(p_i) + \sum_i \frac{\partial F_H^c(p_i)}{\partial p_i} \Delta p_i + O(\Delta p_i)^2 \qquad (2.26)$$

where the second and higher order terms in p_i are neglected. Let us define

$$D_H(p_i) = \left(|F_H^o| - |F_H^c(p_i)| \right) \qquad (2.27)$$

Now, the equation (2.25) can be expressed in the form:

$$R = \sum_{H} w_H \left\{ D_H(p_i) - \sum_i \frac{\partial F_H^c(p_i)}{\partial p_i} \Delta p_i \right\}^2 \qquad (2.28)$$

To minimize R we set the derivatives of R with respect to each p_i equal to zero. Thus

$$\frac{\partial R}{\partial (\Delta p_j)} = -2 \sum_{H} w_H \left\{ D_H(p_i) - \sum_{i=1}^{n} \frac{\partial F_H^c(p_i)}{\partial p_i} \Delta p_i \right\} \frac{\partial F_H^c(p_i)}{\partial p_j} = 0$$

$$(j = 1, 2, 3, \ldots n) \qquad (2.29)$$

where it is assumed that p_i's are all independent.

Eqn. (2.29) gives n normal equations from which corrections (Δp_i) to n parameters (p_i) can be determined. These normal equations (2.29) can be expressed in matrix form as

$$[A]\,\Delta \underline{p} = \underline{B} \tag{2.30}$$

where the elements of matrix $[A]$ and the components of vector $\underline{B}$ are respectively:

$$\left.\begin{aligned} a_{ij} &= \sum_H w_H \frac{\partial F_H^c(p_i)}{\partial p_i} \frac{\partial F_H^c(p_i)}{\partial p_j} \\ \text{and} \\ b_j &= \sum_H w_H D_H(p_i) \frac{\partial F_H^c(p_i)}{\partial p_j} \end{aligned}\right\} \tag{2.31}$$

The solution of the matrix equation (2.30) is obtained by premultiplying both sides with the inverse matrix $[A^{-1}]$ such that

$$[A^{-1}][A]\,\Delta \underline{p} = \Delta \underline{p} = [A^{-1}]\,\underline{B} \tag{2.32}$$

The diagonal terms of the matrix $[A]$, a_{ii}, will be large being sum of the squares, but the cross terms involving the sum of products $\frac{\partial F_H^c}{\partial p_i}\frac{\partial F_H^c}{\partial p_j}$ which maybe +ve or -ve will be small unless the parameters p_i and p_j are strongly dependent.

The standard errors in the variable parameters, P_j, are computed using the relation (Rollett, 1965; p.113)

$$\sigma(P_i) = \left\{ \frac{\sum w(|F_o| - |F_c|)^2}{(m-n)} (a^{-1})_{ii} \right\}^{\frac{1}{2}} \tag{2.33}$$

where m and n are the number of observations and the number of variables respectively, and the $(a^{-1})_{ii}$'s are the diagonal elements of the inverse matrix $[A^{-1}]$.

CHAPTER 3

PREPARATION OF COMPOUNDS AND THEIR LATTICE CONSTANTS

3.1 Preparation of Compounds:

Ammonium hexabromotellurate, $(NH_4)_2TeBr_6$ and Cesium hexabromotellurate, Cs_2TeBr_6 were prepared using a method similar to that described for the preparation of K_2TeBr_6 and $(NH_4)_2TeCl_6$ in Inorganic Syntheses (1946). Both preparations are based on the following chemical reactions:

$$TeO_2 + 6HBr = H_2TeBr_6 + 2H_2O$$

$$H_2TeBr_6 + 2MBr = M_2TeBr_6 + 2HBr$$

where $M = NH_4, Cs$.

(a) Preparation of $(NH_4)_2TeBr_6$

5 gms of tellurium dioxide (TeO_2) was dissolved in 50ml of 40% hydrobromic acid (HBr). A saturated solution of two molal equivalent of ammonium bromide (NH_4Br) was then added to it. The resulting solution was evaporated on a steam bath and stirred until an orange precipitate was obtained. The precipitate was carefully filtered and then recrystallized from boiling water containing about 5% HBr acid. The crystals of $(NH_4)_2TeBr_6$ obtained on cooling were later dried in a vacuum dessicator over silica gel and finally over concentrated sulfuric acid.

A similar procedure was followed for the preparation of Cs_2TeBr_6. In this case a saturated solution of cesium bromide (CsBr) was used.

Bright red octahedral crystals of $(NH_4)_2TeBr_6$ and Cs_2TeBr_6 thus obtained are quite stable in air at room temperature.

3.2 Determination of Accurate Cell Constants:

The powder photographs of these compounds were taken with Ni-filtered Cu radiation using a Philips Debye-Scherrer powder camera (diameter 114.59mm) designed to the Straumanis method of film mounting (Buerger, 1942; p.395). The specimen in finely powder form was packed in a thin walled silica capillary tube, 0.3mm in diameter, and carefully mounted and centered on the camera.

In the Straumanis method a single strip of film is wrapped round the circumference of the camera and as can be seen in Fig. 4, holes in the film provide means by which the X-ray beam enters and leaves the camera. The positions on the film corresponding to $\theta=0^{\circ}$ and $\theta=90^{\circ}$ can be obtained from the mean position of the centers of pairs of powder lines around the exit and entrance holes respectively. The camera is so designed that a spacing of 2mm on the film corresponds to 1° Bragg angle.

Systematic errors in powder diagrams are caused by eccentricity of the specimen, lack of knowledge of the effective camera radius, shrinkage of the film in the process of development and absorption of the specimen. Buerger (1942; p. 399) discusses in detail these sources of errors and their effects on the positions of powder lines on the film. The errors vanish (or at least reduce appreciably) near to a Bragg angle $\theta=90^{\circ}$, i.e., $2\theta=180^{\circ}$ (the back-reflection region).

Differentiating the Bragg relation, $d=\lambda/(2\sin\theta)$ we obtain (using Δ to denote the derivative),

$$\Delta d = -\frac{\lambda}{2}\frac{\cos\theta}{\sin^2\theta}\,\Delta\theta$$

or

$$\frac{\Delta d}{d} = -\cot\theta\,\Delta\theta \qquad (3.1)$$

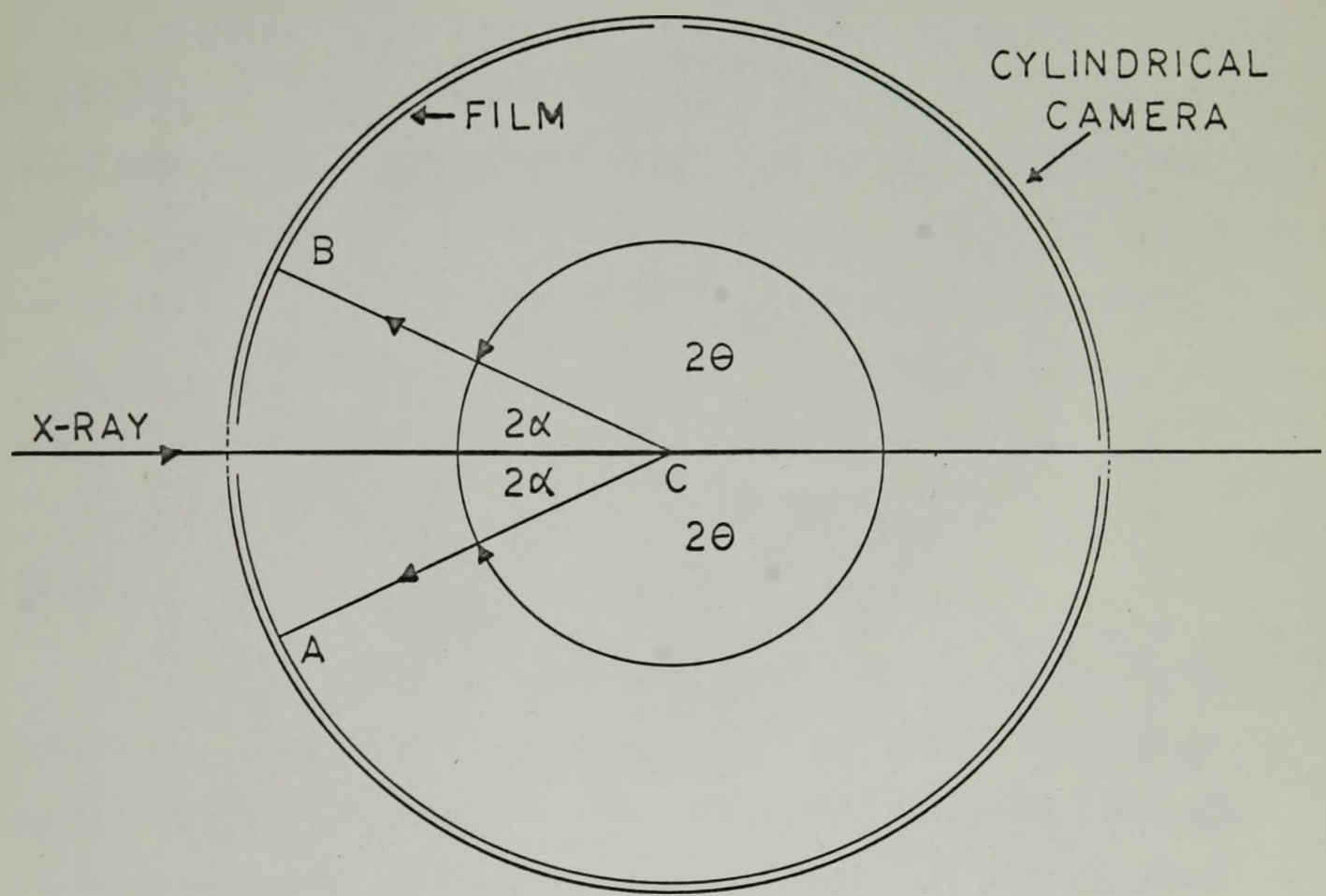

Fig. 4 The Straumanis method of film mounting

Thus a small relative change in interplaner spacing produces a large variation in Θ when $\cot\Theta$ is small, i.e., when Θ approaches 90°, and the limit of resolution in this case is theoretically infinite.

Powder lines at high Bragg angles were utilized in the present work to determine the accurate lattice constants of $(NH_4)_2TeBr_6$ and Cs_2TeBr_6. Powder photographs of each compound were taken with exposures of approximately 40 hours to obtain sufficient lines on the film in the back-reflection region. Usually these lines are very weak. About ten lines close to and on either side of the exit hole were measured. From the differences in readings of each pair the corresponding Bragg angle Θ was calculated. This is illustrated in Fig. 4 where A and B denote the positions of intersections of a diffracted ray cone with the film. It is clear from Fig. 4 that

$$B - A = 4\alpha \quad (B>A)$$

Since

$$4\Theta + 4\alpha = 360^\circ , \quad \Theta = 90^\circ - \alpha$$

The resultant values of Θ and hence $\sin\Theta$ for the reflections can be used to calculate the lattice parameters of a compound. For a cubic crystal, the lattice constant a_o can be determined easily from knowledge of the d-spacing and the Miller indices of each reflection as discussed below.

The d-spacing for any set of planes $H(=hk\ell)$ can be calculated (Section 2.1) using the relation

$$\underline{d}^*_H = h\underline{a}^* + k\underline{b}^* + \ell\underline{c}^* \qquad (3.2)$$

$$|\underline{d}_H| = \frac{1}{|\underline{d}^*_H|} = 1/(\underline{d}^*_H \cdot \underline{d}^*_H)^{\frac{1}{2}}$$

$$= 1/(h^2a^{*2}+k^2b^{*2}+\ell^2c^{*2}+2hka^*b^*\cos\ ^*+2k\ell b^*c^*\cos\alpha^*+2h\ell a^*c^*\cos\beta^*)^{\frac{1}{2}} \tag{3.3}$$

where α^*, β^* and γ^* are angles between b^* and c^* axes, c^* and a^* axes, and a^* and b^* axes respectively.

For cubic crystals, $a^*=b^*=c^*$ and $\alpha^*=\beta^*=\gamma^*=90^\circ$ and hence the equation (3.3) reduces to

$$d_H = \frac{1}{a^*(h^2+k^2+\ell^2)^{\frac{1}{2}}} \tag{3.4}$$

Since $\underline{a} \cdot \underline{a}^* = 1$ (see Section 2.1), $|\underline{a}| = \frac{1}{|\underline{a}^*|}$ (for the cubic crystal). Hence,

$$d_H = \frac{a}{(h^2+k^2+\ell^2)^{\frac{1}{2}}} = \frac{a}{N^{\frac{1}{2}}} \tag{3.5}$$

where $N = (h^2+k^2+\ell^2)$ = an integer.

The observed values of $\sin\theta$ for the powder lines can be used to calculate the d-spacings using the Bragg relation: $2d_H\sin\theta=\lambda$. Combining the equation (3.5) with the Bragg relation we obtain

$$\sin^2\theta_H = A(h^2+k^2+\ell^2) = AN \tag{3.6}$$

where $A = \lambda^2/4a^2$. The common factor A can be evaluated from the $\sin^2\theta_H$ values for the first two powder lines and on dividing other $\sin^2\theta_H$ values by A, the corresponding values of N are obtained.

Thus the cell constant a_o can be calculated using the relation:

$$a_o = d_H\sqrt{N} = \frac{\lambda}{2\sin\theta}\sqrt{N} \tag{3.7}$$

Further, it is seen from (3.7) that

$$\frac{da_o}{a_o} = -\cot\theta d\theta \tag{3.8}$$

Hence, as $\theta \rightarrow 90^\circ$, $\cot\theta \rightarrow 0$, and the error in θ produces vanishingly small error in a_o.

Again, since the α_1 and α_2 components of a reflection are expected to be resolved at high Bragg angles, one should use the corresponding wavelengths for these components separately in calculating the lattice parameter of the sample. But in the powder diagrams of $(NH_4)_2TeBr_6$ and Cs_2TeBr_6 taken with exposure times of 45 hours and 50 hours respectively, the high angle reflections were too weak to identify the α_1 and α_2 doublets distinctly and so the weighted mean wavelength of CuKα radiation (λ=1.54178Å) was used.

Tables II and III list the d-spacings of the powder lines of $(NH_4)_2TeBr_6$ and Cs_2TeBr_6 respectively. The accurate cell constants of $(NH_4)_2TeBr_6$ (Table IV A) and Cs_2TeBr_6 (Table IV B) determined by the method discussed above are in good agreement with the values of Swanson et al. (1957, 1960) (see Table V). The density D_m of each compound was measured by the pycnometer method (International Tables III, 1962; p.18) using carbon tetrachloride, CCl_4, at 20°C. From the knowledge of D_m, the value of Z (number of molecules per unit cell) was determined. The calculated density, D_x was estimated for each compound using the relation (Buerger, 1960; p.243).

$$D_x(gm/cm^3) = \frac{Z \times \text{Formula Weight (a.m.u.)} \times 1.660 \times 10^{-24}}{\text{Volume of unit cell } (Å^3) \times 10^{-24}} \qquad (3.9)$$

The crystal data of $(NH_4)_2TeBr_6$ and Cs_2TeBr_6 are listed in Table V.

TABLE II

The observed and calculated d-spacings for $(NH_4)_2TeBr_6$

The column headings refer to h,k,ℓ , d(observed), d(calculated) and relative intensity (visually estimated)

H	K	L	D(O)	D(C)	INT
1	1	1	6.167	6.194	70
2	0	0	5.354	5.364	95
3	1	1	3.239	3.235	50
2	2	2	3.096	3.097	90
4	0	0	2.686	2.682	100
3	3	1	2.455	2.461	40
4	2	0	2.394	2.399	80
5	1	1	2.067	2.065	40
3	3	3			
4	4	0	1.899	1.896	95
5	3	1	1.809	1.813	40
6	0	0	1.785	1.788	55
4	4	2			
5	3	3	1.633	1.636	20
6	2	2	1.616	1.617	40
4	4	4	1.551	1.548	45
7	1	1	1.500	1.502	20
5	5	1			
6	4	0	1.488	1.488	20
7	3	1	1.396	1.397	20
5	5	3			
8	0	0	1.343	1.341	20
8	2	0	1.300	1.301	25
6	4	4			
6	6	0	1.266	1.264	5
8	2	2			
7	5	1	1.237	1.239	10
5	5	5			
6	6	2	1.229	1.231	10
8	4	0	1.199	1.199	30
9	1	1	1.177	1.178	5
7	5	3			
8	4	2	1.170	1.171	20
9	3	1	1.122	1.125	3
8	4	4	1.094	1.095	20
7	7	1	1.078	1.078	5
9	3	3			
7	5	5			
10	2	0	1.052	1.052	2
8	6	2			
9	5	1	1.039	1.037	5
7	7	3			
10	4	0	0.996	0.996	10
8	6	4			
11	1	1	0.968	0.967	2
7	7	5			
8	8	0	0.949	0.948	5
11	3	1	0.937	0.937	5
9	7	1			
9	5	5			
11	3	3	0.910	0.910	2
9	7	3			
12	0	0	0.894	0.894	5
8	8	4			
11	5	3	0.861	0.862	5
9	7	5			
12	4	0	0.848	0.848	5
10	8	0	0.838	0.838	5
12	4	2			
8	8	6			

TABLE III

The observed and calculated d-spacings for Cs_2TeBr_6

The column headings refer to h,k,ℓ, d(observed), d(calculated) and relative intensity (visually estimated)

H	K	L	D(O)	D(C)	INT
1	1	1	6.177	6.304	30
2	2	0	3.839	3.860	30
3	1	1	3.269	3.292	10
2	2	2	3.132	3.152	100
4	0	0	2.698	2.729	85
3	3	1	2.501	2.505	10
4	2	2	2.227	2.229	30
5	1	1	2.098	2.101	15
3	3	3			
4	4	0	1.924	1.930	75
5	3	1	1.843	1.845	15
6	2	0	1.723	1.726	15
6	2	2	1.643	1.646	50
4	4	4	1.574	1.576	50
7	1	1	1.526	1.529	10
5	5	1			
6	4	2	1.457	1.459	20
7	3	1	1.419	1.421	10
5	5	3			
8	0	0	1.365	1.365	25
8	2	2	1.287	1.287	10
6	6	0			
6	6	2	1.252	1.252	30
8	4	0	1.221	1.221	40
9	1	1	1.199	1.198	4
7	5	3			
6	6	4	1.166	1.164	3
9	3	1	1.144	1.145	3
8	4	4	1.115	1.114	40
10	2	0	1.070	1.071	10
8	6	2			
10	2	2	1.050	1.051	15
6	6	6			
10	4	2	0.997	0.997	1
8	8	0	0.965	0.965	5
10	6	0	0.935	0.936	1
8	6	6			
10	6	2	0.923	0.923	10
12	0	0	0.910	0.910	10
8	8	4			
12	4	0	0.863	0.863	5
10	8	2	0.842	0.842	1
10	6	6	0.833	0.832	2
12	4	4	0.823	0.823	2

TABLE IVA

Accurate lattice constant of $(NH_4)_2TeBr_6$

H	K	L	SINθ(OBS)	LAT.CONST. a_0 (Å)	MEAN a_0 (Å)
10	4	0	0.77384	10.729	
8	6	4			
11	1	1	0.79600	10.740	
7	7	5			
8	8	0	0.81259	10.734	
11	3	1	0.82363	10.713	
9	7	1			
9	5	5			
11	3	3	0.84740	10.726	10.728±0.003
9	7	3			
12	0	0	0.86251	10.726	
8	8	4			
11	5	3	0.89478	10.726	
9	7	5			
12	4	0	0.90887	10.729	
10	8	0	0.91982	10.732	
12	4	2			
8	8	6			

TABLE IVB

Accurate lattice constant of Cs_2TeBr_6

H	K	L	SINθ(OBS)	LAT.CONST. a_0(Å)	MEAN a_0(Å)
10 6	2 6	2 6	0.7341	10.913	
10	4	2	0.7731	10.923	
8	8	0	0.7986	10.921	
10 8	6 6	0 6	0.8241	10.909	
10	6	2	0.8354	10.919	10.919±0.002
12 8	0 8	0 4	0.8472	10.919	
12	4	0	0.8932	10.917	
10	8	2	0.9152	10.918	
10	6	6	0.9258	10.921	
12	4	4	0.9366	10.919	

TABLE V

Crystal data for $(NH_4)_2TeBr_6$ and Cs_2TeBr_6

	$(NH_4)_2TeBr_6$	Cs_2TeBr_6
System	cubic	cubic
F.W.	643.2	872.9
a_o	10.728 ± 0.003Å (1)	10.918 ± 0.002Å (1)
	10.731Å (2)	10.919Å (3)
	10.73 ± 0.02Å (4)	10.910 ± 0.005Å (5)
V	1234.7Å^3	1301.5Å^3
D_m (pycnometric)	3.42 ± 0.02 g cm^{-3}	4.43 ± 0.02 g cm^{-3}
Z	4	4
D_x	3.46 g cm^{-3}	4.45 g cm^{-3}
Absorption coefficient		
for MoK_α	230 cm^{-1}	274 cm^{-1}
for $CuK\alpha$	453 cm^{-1}	860 cm^{-1}
Space group	$Fm3m(O_h^5)$	$Fm3m(O_h^5)$

Systematic absences $hk\ell$: $h+k$, $k+\ell$, $h+\ell = 2n+1$ (both crystals)

---

(1) present work
(2) Swanson et al. (1957)
(3) Swanson et al. (1960)
(4) Manojlović (1957)
(5) Bagnall et al. (1955)

CHAPTER 4

MEASUREMENT OF INTENSITIES

4.1 Size and Shape of Crystal:

For single crystal X-ray diffraction experiments the major consideration which limits the size of the specimen is the absorption of X-rays by the sample. If the absorption coefficient is large, the intensities of reflections are weak unless a very small crystal is used. The intensity of the diffracted beam, I, is given by

$$I = I_o \exp(-\mu t) \qquad (4.1)$$

where I_o is the intensity of the incident beam, t is the effective path length of the rays in the crystal and μ is the linear absorption coefficient. The values of μ for $(NH_4)_2TeBr_6$ and Cs_2TeBr_6 crystals are calculated (Buerger, 1942; p.181) as listed below:

	CuKα	MoKα
$(NH_4)_2TeBr_6$	453 cm^{-1}	230 cm^{-1}
Cs_2TeBr_6	860 cm^{-1}	274 cm^{-1}

using the mass absorption coefficient data from International Tables (Vol. III, 1962; Table 3.2.2A).

Because of low absorption of MoKα radiation in these crystals as compared to CuKα radiation, the former radiation is preferred in single crystal diffraction work. However, if we consider the relative intensities of the diffracted MoKα and CuKα radiations from a crystal of effective thickness t, we find that

$$\frac{I_{Mo}}{I_{Cu}} = \frac{\lambda_{Mo}^3}{\lambda_{Cu}^3} \quad \frac{\exp(-\mu_{Mo}t)}{\exp(-\mu_{Cu}t)} \tag{4.2}$$

where the subscripts Mo and Cu refer to MoKα and CuKα radiations respectively.

Since $\lambda_{Mo} \simeq 0.46\ \lambda_{Cu}$, the expression (4.2) becomes

$$\frac{I_{Mo}}{I_{Cu}} \simeq (0.46)^3 \exp\left[(\mu_{Cu} - \mu_{Mo})t\right] \tag{4.3}$$

Thus for $(NH_4)_2TeBr_6$ and Cs_2TeBr_6 crystals with t about 0.01 cm and 0.004 cm respectively, the ratio of I_{Mo}/I_{Cu} is equal to unity. While with thin crystals Cu-radiation maybe used to get a greater intensity in the diffracted beam, for thicker crystals Mo-radiation is a better choice. Also because of its smaller wavelength, MoKα radiation allows a greater number of reflections to be recorded. This is particularly important when the data are being photographed on a precession camera which only records the diffraction pattern out to a Bragg angle of 30°.

In precession geometry, for a plate shaped crystal of uniform thickness, t, oriented with the X-ray beam incident on the largest face of the crystal, the absorption factor, A, for the zero layer reflections is given by (Buerger, 1964; p.224):

$$A = \frac{I}{I_o} = \exp(-\mu t \sec \bar{\mu}) \tag{4.4}$$

where $\bar{\mu}$ is the precession angle.

For small plate shaped crystal bathed in the incident beam the path lengths of the rays are all equal except for the rays incident on

the small region close to the edges of the crystal for which the path lengths are shorter. Thus, if we neglect this edge effect (which otherwise is difficult to estimate unless the profiles of the crystal edges are known), for all practical purposes, the absorption can be considered uniform for all reflections on the same layer and varies only from layer to layer. For thicker plate shaped crystal the edge effect is significant, since the path lengths of the rays are uniform only over a small region near the centre of the crystal. For a cube shaped crystal, whose shape can be approximated by a sphere, the edge effect is of great importance in estimating the absorption correction which can no longer be considered uniform over the crystal.

For a spherical crystal the absorption correction varies with the Bragg angle (International Tables, Vol. II, 1962; p.302). For crystals with $\mu R < 2$, R being the radius of the sphere, the ratio of the absorption factor, A, for $\theta = 0^\circ$ to that for $\theta = 30^\circ$ is less than 1.5.

The crystals of $(NH_4)_2TeBr_6$ and Cs_2TeBr_6 of approximate dimensions: 0.039 x 0.015 x 0.008 cm and 0.023 x 0.015 x 0.006 cm respectively were selected for single crystal diffraction. These crystals cannot be treated as infinite thin plates where the absorption is constant for all reflections. If the crystal shape is approximated by a sphere the absorption correction for $\theta = 0^\circ$ differs by a factor of about 1.6 from the correction for $\theta = 30^\circ$ for both crystals. Since the crystals were neither plate-shaped nor spherical, but had a shape somewhere between these two extremes, the maximum variation of A for the reflections recorded will be less than 1.6.

The absolute value of the absorption correction is not important, since only the relative intensities of the reflections are measured.

The neglect of the absorption correction to the reflections, however, affects the atomic parameters, especially the thermal parameters of atoms, since the temperature factors (section 2.4A) vary with sinθ in a way similar to the absorption factor (A).

In the present investigation the absorption correction was neglected and justification for neglecting this correction is discussed in Chapter 6.

4.2 Measurement of Intensities:

The single crystal of $(NH_4)_2TeBr_6$ was mounted on a glass fibre attached to a goniometer head and the intensity photographs were taken on a precession camera with the largest face (001) of the crystal perpendicular to the direction of the incident beam. Photographs were taken in five layers each with five different exposures: 1/3, 1, 3, 9 and 27 hours respectively, and the intensities were measured visually using a calibrated wedge. A different procedure was followed for collection of the intensity data from the Cs_2TeBr_6 crystal. Integrated intensity photographs were taken on a Supper Integrated Precession camera for four layers parallel to the largest face (011) of the crystal; each layer was photographed with three different exposures: 3x, 6x, and 9x 2 hours 24 minutes.

To measure the integrated intensities of the reflections, a

Leeds and Northrop microdensitometer was used. From the densitometer traces of the spots, the integrated intensities (section 2.3) of the reflections were estimated. The background of the spots lying on white radiation streaks was measured on the streak. Although the measurements of intensities by microdensitometer is superior to visual estimation, it is not as easy to measure the intensities of relatively weak reflections for which the eye is more sensitive.

4.3 Intensity Corrections and Relative Scaling of Layers:

The observed intensities of the reflections were corrected for the Lorentz and polarization effects (section 2.3). An IBM 7040 program, PRELP, written for this purpose was used to obtain the observed structure amplitudes, $|F_o(\underline{H})|$, of the reflections from different layers from their measured intensities, I(H), using the relation [equation (2.17)]

$$|F_o(\underline{H})|^2 = I(H)/(Lp)$$

where 1/(Lp) is Lorentz-polarization correction factor as given by Jaser (1951) [see also Burbank (1952)] .

The standard errors in $|F_o(\underline{H})|$'s were calculated from an estimate which had been made of the standard errors of the intensities, I(H). In visual estimation of intensities (used only for the reflections recorded from $(NH_4)_2TeBr_6$ crystal), (i) those reflections which are measured from two or more films had their standard errors estimated from the spread of their intensity values (which were usually of the order of 10% to 15% of

the respective intensities); (ii) those reflections, especially some very strong reflections, which were measured from only one film had standard errors of 20% to 25% assigned to them; and (iii) some very weak reflections whose measurement was not very accurate due to large background, irregularity in spot shape etc., had standard errors of up to 50% assigned to them.

For reflections from the Cs_2TeBr_6 crystal, where the integrated intensities were measured from microdensitometer traces, standard errors of the order of 5% to 10% were estimated from measurement of the intensities from three films. However, to some very strong reflections which could only be measured from one film with the shortest exposure, a standard error of 15% was assigned.

For the unobserved reflections* in both methods of estimation of the intensities, a scheme similar to that proposed by Hamilton (1955) was used. The intensity of an unobserved reflection was considered equal to $I_{min}/3$, where I_{min} denotes the background intensity at the location of the spot on the film, and a standard error of $2/3\ I_{min}$ was assigned to it.

Scaling of layers: Because of the cubic symmetry of the crystals, some reflections in higher layers were equivalent to those in lower layers, and thus the intensity data from different layers could be scaled to each other. However, it was not possible with the layers measured for the $(NH_4)_2TeBr_6$ crystal to scale the intensity data from layers in which h, k and ℓ were all odd with those in which h, k and ℓ were all even.

---

*Unobserved on the film, because the intensities of the reflections are very weak compared to the background at the respective spot location.

CHAPTER 5

STRUCTURE ANALYSIS AND REFINEMENT

Previous work on $(NH_4)_2TeBr_6$ and Cs_2TeBr_6 by Monojlović (1957) and Bagnall et al. (1955) respectively show that both crystals are isomorphous with K_2PtCl_6 (Ewing and Pauling, 1928), in which the atoms lie in special positions in the unit cell as noted below (International Tables, Vol. I, 1958; p.538):

<u>Space group $Fm\bar{3}m$ (O_h^5)</u>

Pt in 4(a): (0,0,0); etc.

Cl in 24(e): (x,0,0); etc. with x=0.24

K in 8(c): (1/4,1/4,1/4); etc.

In $(NH_4)_2TeBr_6$ and Cs_2TeBr_6, the positions of Te, Br and N or Cs atoms are same as that of Pt, Cl and K respectively in the K_2PtCl_6 structure. The scattering of X-rays by the hydrogen atoms is very small since they each contain only one electron, and so in the structure factor calculation for $(NH_4)_2TeBr_6$ their contributions were neglected.

5.1 Structure Factor Calculation:

Since $(NH_4)_2TeBr_6$ and Cs_2TeBr_6 both have similar structures, only the structure factor expression for the $(NH_4)_2TeBr_6$ crystal is derived below. The same expression also applies for the Cs_2TeBr_6 crystal.

In general, the structure factor (Eqn. (2.18)) of a reflection with indices $\underline{H}(=h,k,\ell)$ is given by

$$F_c(\underline{H}) = \sum_j f_j T_j \cos 2\pi(hx_j + ky_j + \ell z_j) \tag{5.1}$$

where T_j is the temperature factor of the jth atom in the unit cell and can be expressed as

$$T_j = \exp\left[-(\beta_{11}h^2 + \beta_{22}k^2 + \beta_{33}\ell^2 + 2\beta_{12}hk + 2\beta_{23}k\ell + 2\beta_{13}h\ell)\right] \tag{5.2}$$

where the values of β will depend on the jth atom.

Let us now consider the contributions of the Te, Br and N atoms to the structure factor $F_c(\underline{H})$ separately. A molecule of $(NH_4)_2TeBr_6$ is located around a lattice point such that the Te atom is at (0,0,0) and the whole molecule is centrosymmetric about this position. Thus we will consider here only the atoms present in half of the molecule i.e., NTe_1Br_3, for the present calculation.

The site symmetry of the Te atom is octahedral (m3m), which is a subgroup of the cubic symmetry. Hence the structure factor contribution of the Te atom must be invariant under the reversal of sign and permutation of each of the indices h, k and ℓ, and the conditions are

$$\beta_{11} = \beta_{22} = \beta_{33} = \beta_{11}^{(1)}$$

and

$$\beta_{12} = \beta_{23} = \beta_{13} = 0 \tag{5.3}$$

where the superscript (1) refers to the Te atom. The temperature factor of the Te atom, T_1 is given by

$$T_1 = \exp\left[-\beta_{11}^{(1)}(h^2+k^2+\ell^2)\right] \tag{5.4}$$

and the structure factor contribution can be calculated using the relation:

$$F_1 = \tfrac{1}{4} f_1 T_1 \text{ (Trig 1)}$$

The Te atom being at (0,0,0),

$$\text{Trig 1} = \cos 2\pi(h.0 + k.0 + \ell.0) = 1 .$$

Thus,

$$F_1 = \tfrac{1}{4} f_1 T_1$$

$$= \tfrac{1}{4} f_1 \exp\left[-\beta_{11}^{(1)} (h^2+k^2+\ell^2)\right] \qquad (5.5)$$

The nitrogen atom is at (1/4,1/4,1/4) and the site symmetry is tetrahedral ($\bar{4}3m$), which is a subgroup of the cubic symmetry. Again, since the structure factor contribution of the N atom should be invariant under the reversal of the sign and permutation of each index, the following conditions must be satisfied.

$$\beta_{11} = \beta_{22} = \beta_{33} = \beta_{11}^{(3)}$$

and (5.6)

$$\beta_{12} = \beta_{23} = \beta_{13} = 0$$

where the subscript (3) denotes the nitrogen atom. Thus,

$$F_3 = f_3 T_3 \text{ (Trig 3)}$$

where

$$\text{Trig 3} = \cos 2\pi(h\,1/4 + k\,1/4 + \ell\,1/4) = \cos \tfrac{\pi}{2}(h+k+\ell)$$

and

$$T_3 = \exp\left[-\beta_{11}^{(3)}(h^2+k^2+\ell^2)\right]$$

Hence F_3 can be expressed by

$$F_3 = f_3 \cos \tfrac{\pi}{2}(h+k+\ell) \exp\left[-\beta_{11}^{(3)} (h^2+k^2+\ell^2)\right] \qquad (5.7)$$

The bromine atom, located at (x,0,0), has a tetragonal (4mm) site

symmetry where, of the three orthogonal directions, two directions are equivalent but the third is different from them. So the structure factor contribution of the Br atom should be invariant under the reversal of the sign of each of the indices and the permutation of one pair of indices. Hence, we have in this case

$$\beta_{11} \neq \beta_{22} = \beta_{33}$$

and

$$\beta_{12} = \beta_{23} = \beta_{13} = 0 \tag{5.8}$$

There are three Br atoms in half of the molecule and these are related by the three-fold rotation symmetry about the cubic [111] direction. Thus the positions of the Br atoms are (x,0,0), (0,x,0) and (0,0,x), and the corresponding temperature factors are given by

$$\begin{aligned} \text{Br(1):}\quad T_{2a} &= \exp\left[-\left\{\beta_{11}^{(2a)}h^2 + \beta_{22}^{(2a)}(k^2+\ell^2)\right\}\right] \\ \text{Br(2):}\quad T_{2b} &= \exp\left[-\left\{\beta_{22}^{(2b)}k^2 + \beta_{11}^{(2b)}(h^2+\ell^2)\right\}\right] \\ \text{Br(3):}\quad T_{2c} &= \exp\left[-\left\{\beta_{33}^{(2c)}\ell^2 + \beta_{11}^{(2c)}(h^2+k^2)\right\}\right] \end{aligned} \tag{5.9}$$

where the superscripts (2a), (2b) and (2c) represent the three bromine atoms considered above.

Since all bromine atoms are equivalent in the structure, the β's can be equated as

$$\beta_{11}^{(2a)} = \beta_{22}^{(2b)} = \beta_{33}^{(2c)} = \beta_{11}^{(2)} \tag{5.10}$$

and

$$\beta_{22}^{(2a)} = \beta_{33}^{(2a)} = \beta_{11}^{(2b)} = \beta_{33}^{(2b)} = \beta_{11}^{(2c)} = \beta_{22}^{(2c)} = \beta_{22}^{(2)}$$

where the superscript (2) represent the bromine atom.

The contribution of the Br atoms to the structure factor, F_2, is given by

$$F_2 = \sum_{i=1}^{3} f_2 \left\{T_2 \text{ (Trig 2)}\right\}_i$$

$$= f_2(T_{2a} \cos 2\pi hx + T_{2b} \cos 2\pi kx + T_{2c} \cos 2\pi \ell x) \qquad (5.11)$$

Hence the structure factor expression for all atoms in the chosen unit can be expressed as

$$F_c = F_1 + F_2 + F_3$$

$$= \tfrac{1}{2} f_1 T_1 + f_2(T_{2a} \cos 2\pi hx + T_{2b} \cos 2\pi kx + T_{2c} \cos 2\pi \ell x)$$
$$+ f_3 T_3 \cos \tfrac{\pi}{2}(h+k+\ell) \qquad (5.12)$$

5.2 Refinement:

A trial structure of $(NH_4)_2TeBr_6$ was considered with the position of Br atom at (0.250,0,0) and the Te and N atoms at (0,0,0) and (1/4,1/4,1/4) respectively. A rough estimate of the values of β's was made in the following way. We assume that the T_j's are all equal and can be expressed as $\exp(-BS^2)$ where B is the isotropic temperature factor coefficient and S stands for $(\sin\theta/\lambda)$. Then T_j can be taken outside the summation sign in equation (5.1) as it is common for all atoms. The rest of the structure factor

$$F'_c = \sum_j f_j \cos 2\pi(hx_j + ky_j + \ell z_j)$$

can be calculated and this, when multiplied by T_j, should be equal to the observed structure factor, F_o, multiplied by some appropriate scale factor, K.

Hence,

$$K\,|F_o(H)| = |F'_c(H)|\,\exp(-BS^2) \tag{5.13}$$

or,

$$\ln \frac{|F_o(H)|}{|F'_c(H)|} = -\ln K - BS^2 \tag{5.14}$$

Thus if $\ln(|F_o|/|F'_c|)$ is plotted against S^2 for various reflections (hkℓ), the points should lie on a straight line, and from the intercept and slope of the line the values of K and B respectively can be obtained. The value of $B(=2.0\text{Å}^2)$ so obtained in the present work was used to estimate the β's from the relation (Cruickshank, 1956):

$$4\beta_{ij} = \underline{a}^*_i \cdot \underline{a}^*_j \; B \tag{5.15}$$

where $i,j = 1,2,3$, and $a^*_1 = a^*$, $a^*_2 = b^*$ and $a^*_3 = c^*$.

The trial parameters were refined by a full matrix least squares analysis (section 2.5) of the three dimensional intensity data using the IBM 7040 program MACLS[a]. This program makes use of a special subroutine, CALC, which calculates the structure factors and their derivatives for the particular space group or problem for which it is being used.

In the present work a special subroutine was prepared for crystals with the K_2PtCl_6 structure (space group Fm3m). The variable parameters included in this program were the scale constants applied to the observed structure factors from layers photographed separately, the positional coordinate of the Br atom and the anisotropic temperature factors of all atoms in the unit cell.

---

[a] The program, MACLS, was written in this laboratory by Mr. J. S. Stephens.

The derivatives of $F_c(\underline{H})$ (Eqn. 5.12) with respect to the variable parameters are calculated as noted below.

$$\frac{\partial F_c}{\partial \beta_{11}^{(1)}} = -\tfrac{1}{2} f_1 (h^2+k^2+\ell^2) T_1 \tag{5.16}$$

$$\frac{\partial F_c}{\partial x^{(2)}} = -f_2\, 2\pi (hT_{2a} \sin 2\pi hx + kT_{2b} \sin 2\pi kx + T_{2c} \sin 2\pi \ell x) \tag{5.17}$$

$$\frac{\partial F_c}{\partial \beta_{11}^{(2)}} = -f_2\, (h^2 T_{2a} \cos 2\pi hx + k^2 T_{2b} \cos 2\pi kx + \ell^2 T_{2c} \cos 2\pi \ell x) \tag{5.18}$$

$$\frac{\partial F_c}{\partial \beta_{22}^{(2)}} = -f_2 \left[(k^2+\ell^2) T_{2a} \cos 2\pi hx + (h^2+\ell^2) T_{2b} \cos 2\pi kx + (h^2+k^2) T_{2c} \cos 2\pi \ell x \right] \tag{5.19}$$

$$\frac{\partial F_c}{\partial \beta_{11}^{(3)}} = -f_3\, (h^2+k^2+\ell^2) T_3 \cos \tfrac{\pi}{2}(h+k+\ell) \tag{5.20}$$

and

$$\frac{\partial F_c}{\partial (\text{scale})} = F_c \tag{5.21}$$

The atomic scattering factors for all atoms except hydrogen, which was not included at any stage, were taken from the International Tables (Vol III, 1962)*. The least squares refinement of the three dimensional intensity data of the $(NH_4)_2TeBr_6$ crystal was carried out for six cycles after which no significant changes in the variable parameters were observed. The agreement between the observed and calculated structure factors was checked after each cycle of refinement from the value of the residual index (commonly called the R-factor) of the form:

---

*See International Tables (1962), Vol III, Tables 3.3.1A and 3.3.1B

$$R = \left\{ \frac{\sum w(|F_o| - |F_c|)^2}{\sum w|F_o|^2} \right\}^{\frac{1}{2}} \qquad (5.22)$$

where the summation extends over all reflections.

The weight, w, used in the eqn. (5.22) is given by $w = \frac{1}{\sigma^2}$, where σ is the standard error of the observed structure factor, F_o (see section 4.2). The R-factor after the final cycle of refinement was 0.079. The atomic parameters of $(NH_4)_2TeBr_6$ derived from the final cycle of refinement are listed in Table VI, and the observed and calculated structure factors are given in Table VII.

In the refinement of the crystal structure of Cs_2TeBr_6 the above procedure was also followed. In this case, the atomic parameters of $(NH_4)_2TeBr_6$ obtained after the final cycle of refinement were used as trial parameters and the R-factor after the final refinement of the parameters was 0.082. The positional and thermal parameters of atoms in Cs_2TeBr_6 are given in Table VI and the observed and calculated structure factors are listed in Table VIII.

TABLE VI

Atomic parameters derived from the final least-squares refinement

Crystal	Atom	Positional Coordinates	Temperature factor [b]
$(NH_4)_2TeBr_6$	Te in 4(a)[a]	(0,0,0; etc.)	β_{11} $(=\beta_{22} = \beta_{33}) = 42 \pm 1$
	Br in 24(e)	(x,0,0; etc.) with $x = 0.2499 \pm 0.0002$	$\beta_{11} = 37 \pm 2$; $\beta_{22}(=\beta_{33}) = 134 \pm 1$
	N in 8(c)	$(\frac{1}{4},\frac{1}{4},\frac{1}{4}$; etc.)	β_{11} $(=\beta_{22} = \beta_{33}) = 118 \pm 22$
Cs_2TeBr_6	Te in 4(a)	(0,0,0; etc.)	β_{11} $(=\beta_{22} = \beta_{33}) = 69 \pm 4$
	Br in 24(e)	(x,0,0; etc.) with $x = 0.2468 \pm 0.0004$[c]	$\beta_{11} = 53 \pm 7$; $\beta_{22}(=\beta_{33}) = 106 \pm 1$
	Cs in 8(c)	$(\frac{1}{4},\frac{1}{4},\frac{1}{4}$; etc.)	B_{11} $(=\beta_{22} = \beta_{33}) = 94 \pm 3$

a See International Tables for X-ray Crystallography Vol. I, 1962. p.338.

b The anisotropic temperature factors appear in the structure factor calculation as

$$\exp\left(-10^{-4}(\beta_{11}h^2 + \beta_{22}k^2 + \beta_{33}\ell^2)\right)$$

c The value of x given by Bagnall et al. (1955) is 0.24.

TABLE VII

The observed and calculated structure factors for $(NH_4)_2TeBr_6$

H	K	L	|F(Ø)|	F(C)	H	K	L	|F(Ø)|	F(C)
2	0	0	376	381	6	2	2	255	-261
4	0	0	714	772	8	2	2	93	88
6	0	0	211	181	10	2	2	98	-99
8	0	0	456	393	12	2	2	89	90
10	0	0	38	45	14	2	2	31	-29
12	0	0	180	177	16	2	2	59	57
2	2	0	< 20	-19	4	4	2	278	267
4	2	0	344	313	6	4	2	< 13	10
6	2	0	29	-23	8	4	2	193	183
8	2	0	213	213	10	4	2	< 15	-3
10	2	0	26	-22	12	4	2	107	107
12	2	0	124	126	14	4	2	< 17	-4
14	2	0	< 18	-14	16	4	2	49	55
16	2	0	59	65	6	6	2	137	-149
4	4	0	540	590	8	6	2	64	56
6	4	0	178	166	10	6	2	41	-52
8	4	0	330	321	12	6	2	69	62
10	4	0	51	49	8	8	2	135	122
12	4	0	141	147	10	8	2	30	26
14	4	0	< 17	5	12	8	2	77	68
16	4	0	63	64	3	3	3	*	140
6	6	0	< 29	-15	5	3	3	118	120
8	6	0	132	129	7	3	3	107	97
10	6	0	< 16	-6	9	3	3	76	77
12	6	0	73	83	11	3	3	62	57
8	8	0	174	186	13	3	3	43	43
10	8	0	40	51	5	5	3	113	105
12	8	0	98	88	7	5	3	83	86
1	1	1	*	196	9	5	3	66	69
3	1	1	167	171	11	5	3	48	52
5	1	1	140	141	13	5	3	35	39
7	1	1	117	111	7	7	3	60	72
9	1	1	101	87	9	7	3	57	58
11	1	1	62	64	11	7	3	35	45
13	1	1	46	48	13	7	3	35	34
3	3	1	152	154	9	9	3	49	48
5	3	1	129	130	11	9	3	43	37
7	3	1	100	104	4	4	4	612	469
9	3	1	86	81	6	4	4	149	151
11	3	1	59	61	8	4	4	272	263
13	3	1	40	45	10	4	4	44	50
5	5	1	103	113	12	4	4	136	123
7	5	1	95	92	14	4	4	< 17	10
9	5	1	69	73	16	4	4	54	54
11	5	1	52	55	6	6	4	< 12	8
13	5	1	38	41	8	6	4	108	114
7	7	1	82	76	10	6	4	< 15	6
9	7	1	57	61	12	6	4	69	72
11	7	1	38	47	14	6	4	17	4
13	7	1	26	36	8	8	4	133	155
9	9	1	65	50	10	8	4	48	47
11	9	1	47	39	12	8	4	71	74
13	9	1	33	29					
2	2	2	378	-496					
4	2	2	39	31					

*Unobservable on the precession films due to beam stop.

TABLE VIII

The observed and calculated structure factors for Cs_2TeBr_6

H	K	L	|F(O)|	F(C)	H	K	L	|F(O)|	F(C)
2	0	0	< 35	37	4	4	2	< 59	43
4	0	0	920	1062	6	4	2	166	154
6	0	0	< 54	-5	8	4	2	< 72	45
8	0	0	526	540	6	6	2	308	-313
10	0	0	< 58	-24	8	6	2	100	109
12	0	0	216	218	10	6	2	149	-143
2	2	0	328	305	8	8	2	< 60	37
4	2	0	77	40	3	3	3	143	103
6	2	0	168	174	5	3	3	116	107
8	2	0	52	48	7	3	3	61	57
4	4	0	747	822	9	3	3	51	67
6	4	0	< 56	7	5	5	3	110	106
8	4	0	449	443	7	7	3	< 42	34
10	4	0	< 80	-14	4	4	4	703	659
12	4	0	183	182	6	4	4	< 53	14
6	6	0	115	108	8	4	4	342	365
8	8	0	263	254	10	4	4	< 60	-7
1	1	1	234	209	12	4	4	154	153
3	1	1	184	162	6	6	4	100	98
5	1	1	152	156	8	6	4	< 86	24
7	1	1	73	84	10	6	4	< 94	42
9	1	1	76	91	8	8	4	207	211
3	3	1	128	128	5	5	5	107	101
5	3	1	133	129	7	5	5	58	62
7	3	1	66	69	7	7	5	< 42	37
5	5	1	125	125	6	6	6	225	-208
7	5	1	63	72	8	6	6	73	73
7	7	1	< 59	41	10	6	6	100	-96
2	2	2	800	-815	8	8	6	< 59	21
4	2	2	264	255	7	7	7	< 42	22
6	2	2	435	-482	8	8	8	138	125
8	2	2	139	168					
10	2	2	191	-213					
12	2	2	87	91					

CHAPTER 6

DESCRIPTION OF THE STRUCTURES

The results of the refinement described in section 5.3 confirm that the $TeBr_6^{2-}$ ion has the configuration of a regular octahedron in both $(NH_4)_2TeBr_6$ and Cs_2TeBr_6, and the mean Te-Br bond distances are 2.681±0.002 Å and 2.695±0.004 Å respectively. Cruickshank (1956b) has pointed out that the measured bond lengths are usually shorter than their correct lengths. Since the atoms constituting the bonds are always in thermal motion, the positions of maxima in the electron density distribution donot represent the correct positions of atoms and so the measured bond lengths should be corrected for the thermal motion of atoms constituting the bonds.

Recently Busing and Levy (1964) have proposed a method for correcting the bond distances based on one of the following assumptions regarding the joint electron density distribution of two atoms forming the bond.

(1) The motions of the atoms are either in phase or out of phase with one another.

(2) The motion of the heavier atom is completely independent of the motion of the lighter one, but the lighter atom is supposed to 'ride' on the heavier atom.

(3) There is no correlation between the motions of the atoms.

The first assumption gives the two extreme limits of the bond length; but the other two represent more physically likely situations. It is hard to distinguish between them unless detailed information about the motion of the atoms is known. The root mean square (r.m.s) amplitude of thermal vibration of an atom, $(\overline{u^2})^{\frac{1}{2}}$, normal to the reflecting plane can be calculated (Cruickshank, 1956a) from the relation

$$B = 8\pi^2 \overline{u^2} \qquad (6.1)$$

where B is the isotropic temperature coefficient. For anisotropic motion of the atom the following relation is used to replace B by β's (see equation (5.15))

$$B_{ij} = 4\beta_{ij}/(a_i^* \cdot a_j^*) \qquad (6.2)$$

In the present work it is observed that the Br atoms have large thermal anisotropy with the r.m.s. amplitude of vibration perpendicular to the Te-Br bond significantly larger than that along the bond (see Table IX). A rigid $TeBr_6^{2-}$ ion librating about the central Te atom would give rise to an anisotropy of this sort and if this were the case, the true Te-Br bond distance corrected for the temperature effects would be 2.70Å in both crystals. However, the Te-Br bond length can also be corrected for the thermal effects considering that there is no correlation between the motions of the Te and Br atoms. The thermal anisotropy of the Br atoms can be explained in this case, if we consider that the bending modes of vibration of the Te-Br bond have larger amplitudes than the stretching modes. The corrected Te-Br bonds are then 2.72Å

and 2.73Å in $(NH_4)_2TeBr_6$ and Cs_2TeBr_6 respectively. However, it is not possible to distinguish between the two cases discussed above and the true situation probably lies somewhere between the two extremes.

Further, it is interesting to see that the size of the $TeBr_6^{2-}$ ion is the same in both the crystals in the present study, and is not significantly different from that observed in K_2TeBr_6 (Brown, 1964). Hence it can be presumed that changing the cation does not have a large influence on the structure of the anion in $M_2^{I}TeBr_6$ crystals.

Corrections have been made to other interatomic distances for thermal effects on the assumption that there is no correlation between their motions. But the uncorrected and corrected values of these distances are listed in Table IX. Owing to the uncertainty in the absolute value of the amplitudes of thermal motions and the proper way to correct for for them, the standard error in these distances is estimated to be about 0.01Å . The effects of neglecting absorption correction to the intensity data of these crystals are not significant. The r.m.s. amplitudes of vibration of the atoms change by about 0.005Å if the absorption effect is included, which is less than standard error in the interatomic distances.

The observed M-Br ($M=NH_4$,Cs) distances can be compared with those predicted from the sum of the ionic radii. The ionic radii of Cs and Br listed below have been obtained by correcting Pauling's values (Pauling, 1960; p.511) for twelve coordination.

Ion	Radius (Å)
NH_4^+	1.56
Cs^+	1.80
Br^+	2.10

The ionic radius of NH_4^+ (1.56A) has been estimated by reducing the corrected value of Pauling's ionic radius of Rb^+ (1.60A) in accordance with the observation that crystals of $(NH_4)_2MX_6$(X=Cℓ,Br) all have slightly smaller cells than the corresponding Rb-compounds (Engel, 1935).

The observed (NH_4)-Br distance (3.82Å) is considerably longer than that predicted (3.66Å) but the Cs-Br distance (3.89Å) is the same as that expected from the sum of their ionic radii (3.90Å). Likewise, the distance between Br atoms in different anions are different in the two crystals (3.84Å in $(NH_4)_2TeBr_6$ and 3.94Å in Cs_2TeBr_6) whereas they might be expected to be the same. The probable explanation is that in Cs_2TeBr_6 the Br-Br distances are determined by the fact that the cesium and bromine atoms are in contact (Fig. 5a) so that the anions are just separated, where as in $(NH_4)_2TeBr_6$ it is the bromine atoms in the neighbouring anions that are in contact (Fig. 5b) and the NH_4^+ ion (1.56A) is appreciably smaller than the size of the cavity (1.74A) formed by twelve bromine atoms which surround it. Such a situation, as discussed by Brown (1964), should lead to distortion in the structure at low temperature. A preliminary study of the distortion in $(NH_4)_2TeBr_6$ is discussed in the next chapter.

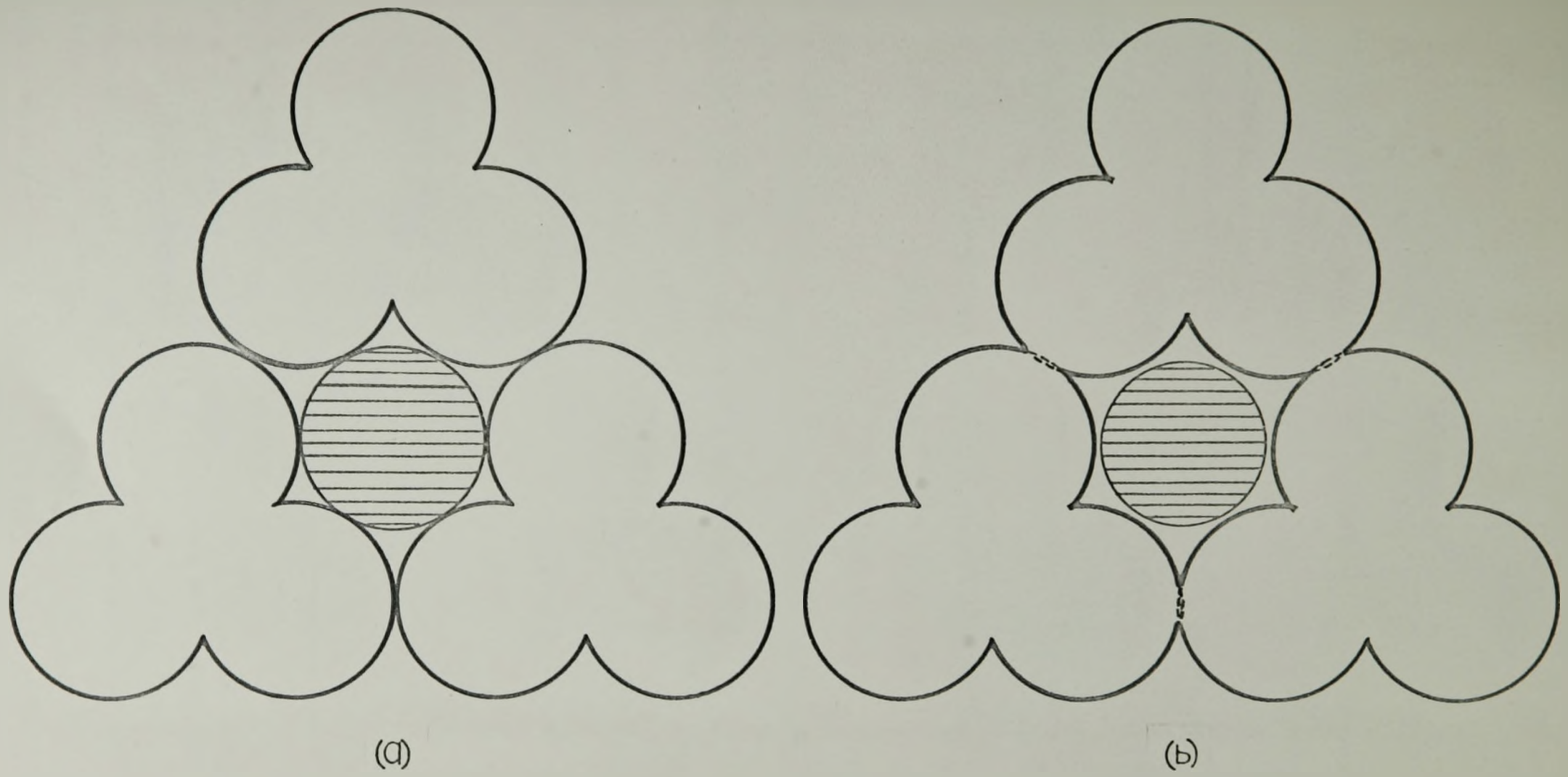

Fig. 5 Sections through the cation perpendicular to (111) direction in (a) Cs_2TeBr_6 and (b) $(NH_4)_2TeBr_6$
Cation (striped circle), Bromine (open circle)

TABLE IX

Interatomic distances and thermal motions in M_2TeBr_6 crystals

	K_2TeBr_6[a]	$(NH_4)_2TeBr_6$	Cs_2TeBr_6
Interatomic distances before correction for thermal motion (Å):			
Te-Br	2.692 ± 0.006[b]	2.681 ± 0.002[b]	2.695 ± 0.004[b]
M-Br		3.793 ± 0.001[b]	3.860 ± 0.001[b]
Br-Br (between anions)		3.794 ± 0.003[b]	3.909 ± 0.003[b]
Interatomic distances after correction for thermal motion (see text) (Å):			
Te-Br	2.71 ± 0.01[c]	2.70 ± 0.01[c]	2.70 ± 0.01[c]
M-Br		3.82 ± 0.01[c]	3.89 ± 0.01[c]
Br-Br (between anions)		3.84 ± 0.01[c]	3.94 ± 0.01[c]
Root mean square amplitudes of thermal vibration (Å):			
Te	0.15[d]	0.16	0.20
Br (i) along TeBr bond	0.14[d]	0.15	0.18
(ii) perpendicular to Te-Br bond	0.25[d]	0.28	0.25
M	0.28[d]	0.26	0.23
Ratio of perpendicular : parallel motion of the bromine atom	1.8	1.9	1.4

a See ref. Brown (1964).

b The error quoted is that calculated from the standard errors indicated for the cell constants and the least-squares refinement and does not include possible systematic errors.

c Estimated standard errors, including an allowance for possible systematic errors.

d Average values.

CHAPTER 7

PHASE TRANSITION IN $(NH_4)_2TeBr_6$

7.1 Introduction:

$(NH_4)_2TeBr_6$ crystals are cubic at room temperature; but, as reported by Nakamura and his co-workers (1962a), they undergo a phase transition at 221°K probably to a phase of tetragonal symmetry. It can be expected that the transformation in this case is similar to that occuring in K_2SnBr_6 (Markstein and Nowotny, 1938), which is tetragonal (with c/a>1) at room temperature but transforms to cubic at 400°K (Galloni et al., 1962). Moreover, the phase transition in K_2SnBr_6 is reversible and the unit cell volume does not change at the transition temperature. This transition is probably of the 'displacive' type in the sense defined by Buerger (1951). Some characteristics of the displacive transition are that the transformation is usually very rapid, since it doesnot involve any disruption of atomic linkages; the network of atoms is only distorted, and the symmetry of the low temperature form is a subgroup of that of the high temperature form.

A mechanism for this type of structural distortion has been proposed by Morfee et al. (1960) for the analogous $(NH_4)_2SnBr_6$ crystal. Here the anions are postulated to rotate about the [001] direction with the alternate (001) layers of anions rotating in the opposite sense. Buerger (1951) has also shown that in displacive transformations, where

the low temperature structure is formed from the high temperature form by loss of symmetry, a down temperature transformation almost invariably results in twins and this is particularly common if the low temperature form has more than one orientation with respect to the high temperature form. Thus in $(NH_4)_2TeBr_6$ crystals twins are likely to be formed from the parent single crystal since there are three possible ways by which the cubic structure can be distorted to a tetragonal form. Unfortunately, a twinned crystal cannot be used easily for complete structure analysis.

The phase transition can be observed in a polarizing microscope (Wahlstrom, 1960; p.127). The theory of this is discussed below. A crystal is placed on the polarizing microscope stage with the polarizer in a crossed position with respect to the analyser. The light emerging from the polarizer is plane polarized with its vibration directions in the plane of vibration of the polarizer, and on entering the crystal it is resolved into two groups of rays - the ordinary (O) ray and the extraordinary (E) ray, both plane polarized at right angles to each other. In general, they travel with different velocities inside the crystal and on emergence the two sets of rays interfere in a manner depending on the magnitude of the path difference and the orientation of the vibration planes of the crystal relative to the vibration plane of the polarizer. The ray emerging from the crystal will have a different direction of polarization from the direction of polarization of the ray incident on the crystal and thus the crystal will appear bright when viewed through an analyser set at right angles to the polarizer. But in some particular

orientations when one of the vibration directions of the crystal is parallel to the plane of vibration of the polarizer, the crystal will appear dark. If the crystal is rotated with respect to the polarizer, such positions will occur 90° apart.

In a cubic crystal, being isotropic, the two sets of rays travel with the same velocity inside the crystal and on emergence no path difference is introduced between these rays. The direction of polarization of the emergent ray does not change with respect to that of the incident ray and thus a cubic crystal will always appear dark when placed between crossed nicols. This fact can be used to observe the phase change between a cubic and a non-cubic phase.

A twinned crystal of the non-cubic phase can also be easily detected, since on examining it between crossed nicols each twin individual will generally be found to extinguish independently, and thus a complete extinction of the whole crystal can not be observed.

7.2 Low Temperature Polarizing Microscope:

A simple low temperature polarizing microscope was designed in this laboratory to serve two purposes: (1) to observe the phase transformation in $(NH_4)_2TeBr_6$ at low temperature, and (2) to help select a single (untwinned) crystal of $(NH_4)_2TeBr_6$.

The schematic diagram of the apparatus is shown in Fig. 6. A pyrex beaker C(150 ml capacity) was placed on the glass base plate B of the microscope. Another smaller beaker D was put inside the beaker C

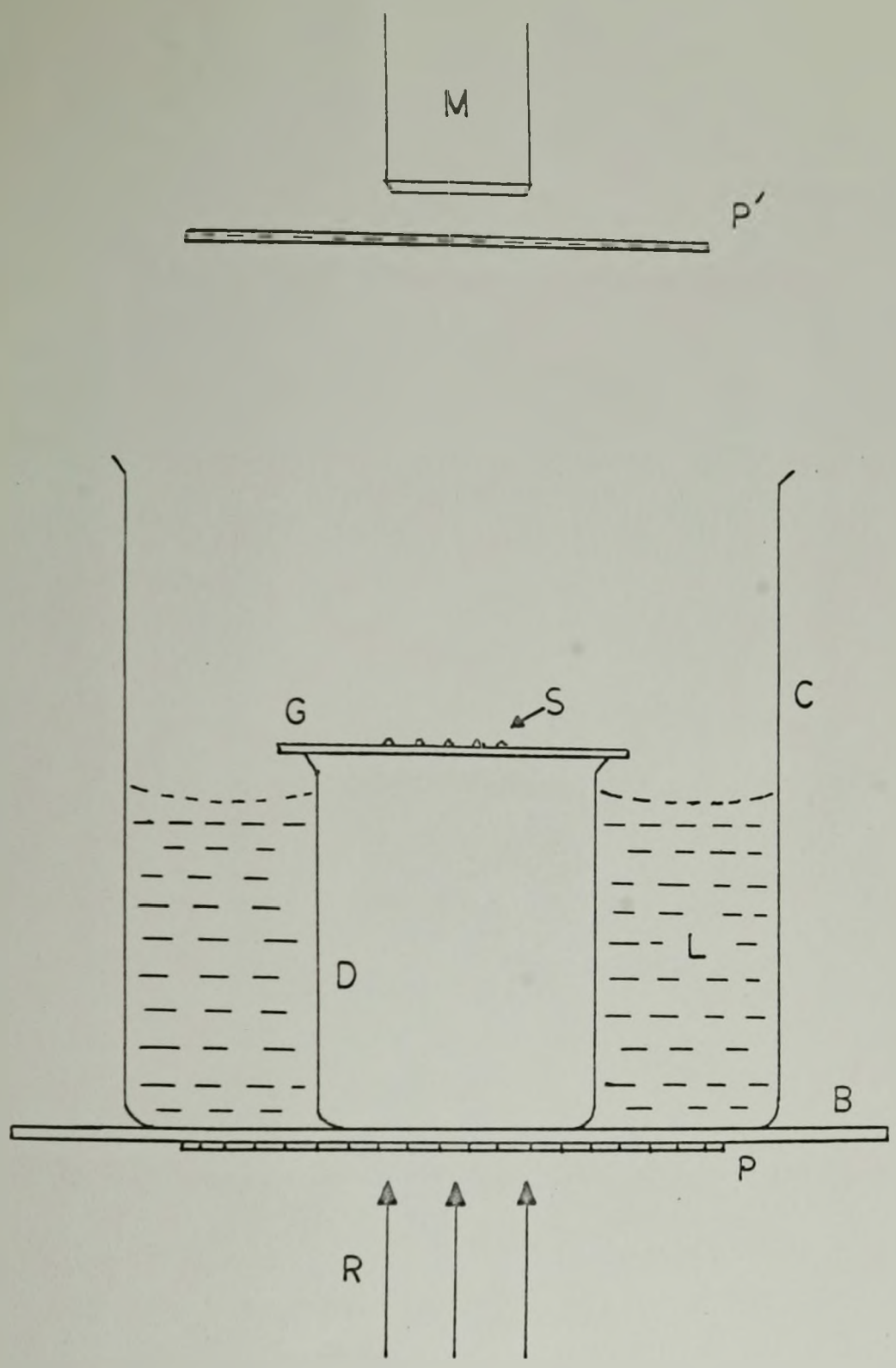

Fig. 6 A schematic view of the low temperature polarizing microscope

with its base glued to that of the latter. A narrow beam of light was used to illuminate the field of view of the microscope from below the base plate B. Two pieces of polaroid sheet were used to serve as the polarizer (P) and the analyser (P') respectively. One of the pieces P was fixed to the bottom surface of the base plate with scotch tape and the other P' was placed in the crossed orientation between the beaker C and the microscope objective M. A small quantity of liquid air was placed in the annular space L between the two beakers and a microscope slide G carrying the sample was placed over the inner beaker D.

So long as the temperature of $(NH_4)_2TeBr_6$ crystals was above the transition temperature they appeared dark between the crossed polaroids, but as soon as the crystals had transformed to a lower symmetry phase on cooling they began to transmit light and, on rotating the beaker C (and hence the sample S), the extinctions could be clearly observed. Although most of the crystals were found to have regions which extinguished independently indicating twins, it was possible to find some single crystals which didnot show twinning below the transition temperature and they were collected for X-ray diffraction studies.

Precautions were taken against the condensation of moisture over the crystals which would otherwise spoil them from further use. So long the sample was inside the beaker C, the air above it was cold and hence dry; but on removing the sample from the beaker moisture rapidly began to condense on the sample, and it was necessary to place the sample in a slow stream of dry and warm air. Moreover, during the experiment the base plate was also kept in a stream of dry air to prevent any ice

formation on the base of the beaker C and the polarizer.

The following observations were also noted during the experiment in connection with the phase transformation of $(NH_4)_2TeBr_6$.

(1) The phase transformation is very rapid.

(2) The bright red colour of $(NH_4)_2TeBr_6$ crystals changes to yellow at low temperature.

(3) On warming up the crystals above the transition temperature, the colour again changes back to red and the crystals revert to the cubic symmetry indicating that the transformation is reversible in nature.

7.3 Measurement of Transition Temperature:

The transition temperature of $(NH_4)_2TeBr_6$ was measured in a Nonius Weissenberg camera designed for X-ray diffraction studies at temperatures between 123°K and 573°K. This equipment was particularly suitable for the present investigation since it was possible to cool the crystal, mounted in the camera by passing cold nitrogen gas over it and the temperature of the gas in the vicinity of the crystal could be measured by a thermocouple.

Two pieces of polaroid were fixed in the crossed position on either side of the layer line screen and connected so that they could both be rotated together. The crystal was viewed through the telescope attached to the Weissenberg camera opposite the collimator, through which a beam of light was passed. Thus when the specimen was cooled

below the transition temperature, the extinction pattern characteristic of non-cubic crystals could be observed. The temperature at which $(NH_4)_2TeBr_6$ crystal just begins to transmit light during cooling or just stops transmitting on warming was measured using a copper-constantan thermocouple calibrated at three standard temperatures e.g., melting ice (273°K), dry ice-acetone mixture (196°K) and the liquid nitrogen (77°K) temperatures. The transition temperature was found to be 183±5°K.

7.4 Weissenberg Photographs and their Interpretation:

To study the symmetry and cell constants of $(NH_4)_2TeBr_6$ below the transition temperature the compound Weissenberg photographs (Figs. 7a and 7b) were taken with two specimens in different orientations. In each case, a low temperature photograph was first taken at about 163°K and then shifting the film to the right by a small amount another photograph was taken at room temperature with the same exposure time.

Fig. 7a shows the compound photograph of a $(NH_4)_2TeBr_6$ crystal of nearly cylindrical shape, radius about 0.008 cm. This photograph was taken with the $[1\bar{1}0]$ direction as the rotation axis of the goniometer. The crystal was realigned at low temperature viewing it against the incident beam direction first by rotating it clockwise about the incident beam by 10' and then about an axis normal to the incident beam clockwise by 20' as viewed from above. In this photograph three principal cubic lattice directions [001], [111] and [110] are seen. The split spots

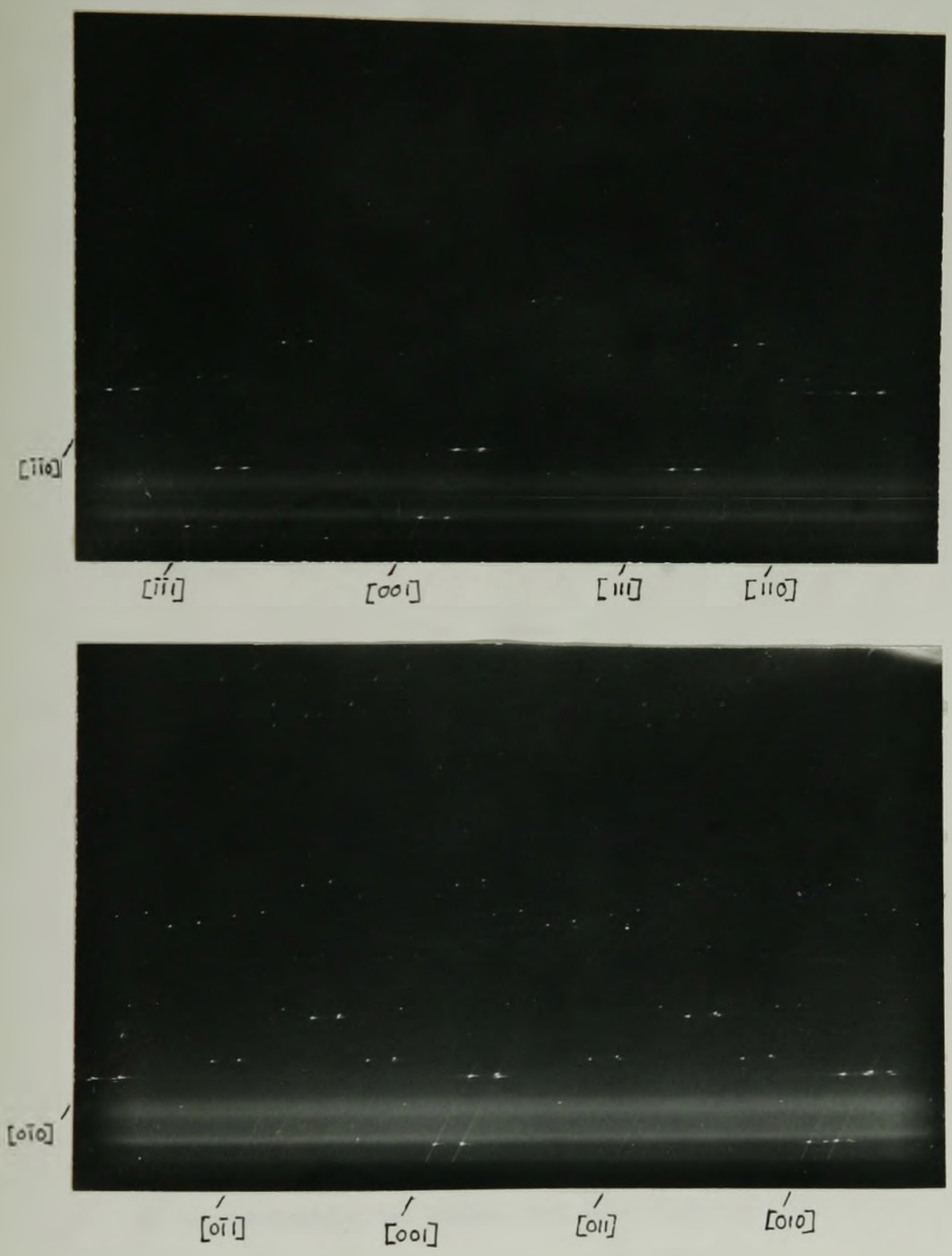

(a)

(b)

Fig. 7 Compound Weissenberg photographs of $(NH_4)_2TeBr_6$ taken at $163^{\circ}K$ and $298^{\circ}K$ about (a) $[1\bar{1}0]$ as rotation axis, and (b) $[100]$ as rotation axis

along the 001 direction in the low temperature phase indicate that twinning in this case is such that C* and A* axis [1] of two twins of the low temperature structure lie along the same direction. The low temperature reflections along the [111] direction donot show any vertical splitting, although their shape suggests that they are probably split horizontally, but are so close that, due to overlapping, their individual identity cannot be distinguished. However, the absence of any obvious splitting of the (111) reflections indicates that the angles α^*, β^* and γ^* are still 90° in the low temperature form, since from the equation (3.3)

$$d^*(hkl) = (h^2a^{*2}+k^2b^{*2}+l^2c^{*2} + 2hka^*b^* \cos \gamma^* + 2klb^*c^* \cos \alpha^* + 2lhc^*a^* \cos \beta^*)^{\frac{1}{2}}$$

and hence

$$d^*(111) = d^*(11\bar{1}) = d^*(1\bar{1}1) = d^*(\bar{1}11)$$

only if the cross terms are zero i.e.,

$$\cos \alpha^* = \cos \beta^* = \cos \gamma^* = 0$$

or

$$\alpha^* = \beta^* = \gamma^* = 90^\circ$$

It is possible to index the low temperature spots on the film assuming that the crystal is tetragonal with $\frac{C}{A} > 1$ and the photographs

---

[1] Capital letters are used here to differentiate the face centered tetragonal cell from the primitive cell for which lower case letters are used.

of the twins correspond to the $(1\bar{1}0)$ and $(0\bar{1}1)$ projections.

Fig. 7b shows a compound photograph of another specimen of cube shape (edge length about 0.008 cm) in the (001) and (100) projections of the low temperature phase. This photograph was taken with the rotation axis of the goniometer along the cubic 100 direction and no realignment of the crystal was made at low temperature. Each pair of spots on the low temperature photograph is seen not only to split vertically, but the lower component of each pair is also displaced horizontally. Further, the reflections along the 010 direction are all single indicating that 010 is the twin axis. It can also be seen that the (0K0) reflections are located at the same Bragg angle on the film as the corresponding (H00) reflections. Hence the A and B axes of the low temperature phase are equal in length and this is consistent with the hypothesis that the low temperature phase is tetragonal.

In Fig. 7b some extra spots are also seen at the lower end of the 010 direction on the film. These can not be indexed on any simple cell and their presence is probably due to some crystallite attached to the specimen. All other spots on the film can be indexed as either (HK0) or (0KL) reflections on the basis of a C-face centred pseudo-cubic tetragonal cell. However, it is normal to index such reflections on the basis of the primitive cell obtained from the pseudo-cubic cell by setting the a axis along the cubic [110] direction, b along the cubic $[\bar{1}10]$ direction and c along the cubic [001] direction (see Fig. 8a).

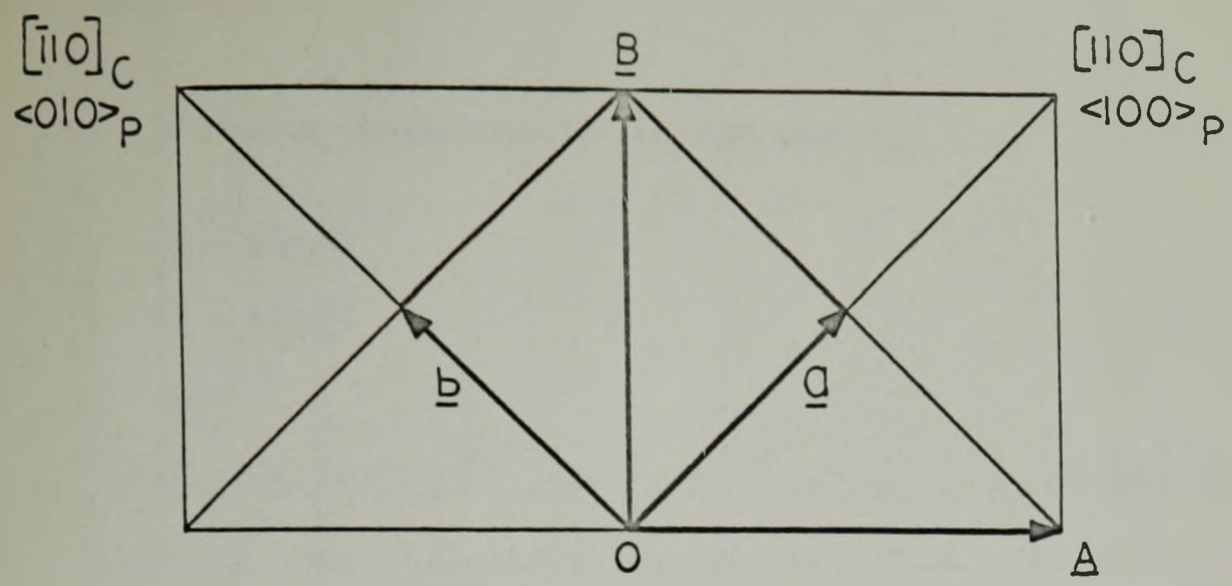

Fig. 8a Transformation of the C-face centered tetragonal cell to a primitive cell

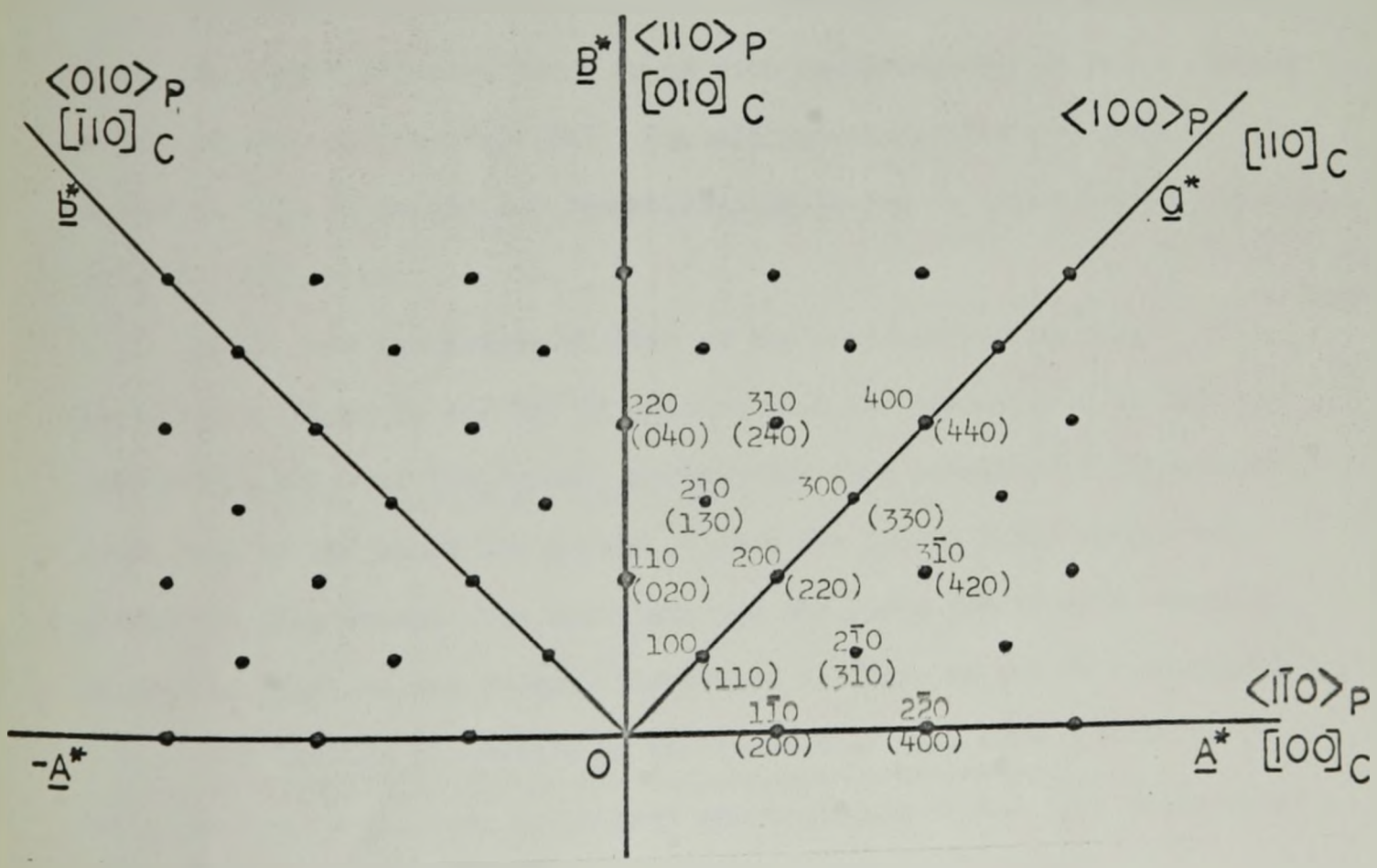

Fig. 8b Reciprocal lattice: C-face centered and primitive tetragonal cell indexings.
The indices for the C-centred cell are given in parentheses.

The axial transformation in this case is:

$$\underline{a} = \tfrac{1}{2}(\underline{A}+\underline{B})$$
$$\underline{b} = \tfrac{1}{2}(\underline{B}-\underline{A}) \qquad (7.2)$$
$$\underline{c} = \underline{C}$$

and the indices (HKL) of a plane in C-centred pseudo-cubic cell can be expressed in terms of the primitive lattice indices h, k, and ℓ, where they are related by the transformation:

$$h = \tfrac{1}{2}(H+K)$$
$$k = \tfrac{1}{2}(K-H) \qquad (7.3)$$
$$\ell = L$$

Since H+K=2n, an even number, all (HKO) reflections with H+K=2n+1 (odd) are absent whereas there is no such condition for the corresponding (hk0) reflections (see Fig. 8b). The additional reflections which appear in Fig. 7b in the low temperature phase can be indexed satisfactorily as (HKO) reflections.

Thus from the interpretation of the compound Weissenberg photographs (Figs. 7a and 7b) it appears that the twinning in the low temperature phase of $(NH_4)_2TeBr_6$ corresponds to a rotation of the pseudo-cubic cell by 90° about the B-axis so that the C-axis falls along the A-axis and vice versa. The splittings of the spots due to such twinning as seen in Figs. 7a and 7b are illustrated in Figs. 9a and 9b respectively.

The lattice parameters of the tetragonal cell were calculated using the low temperature splittings corresponding to the five reflections

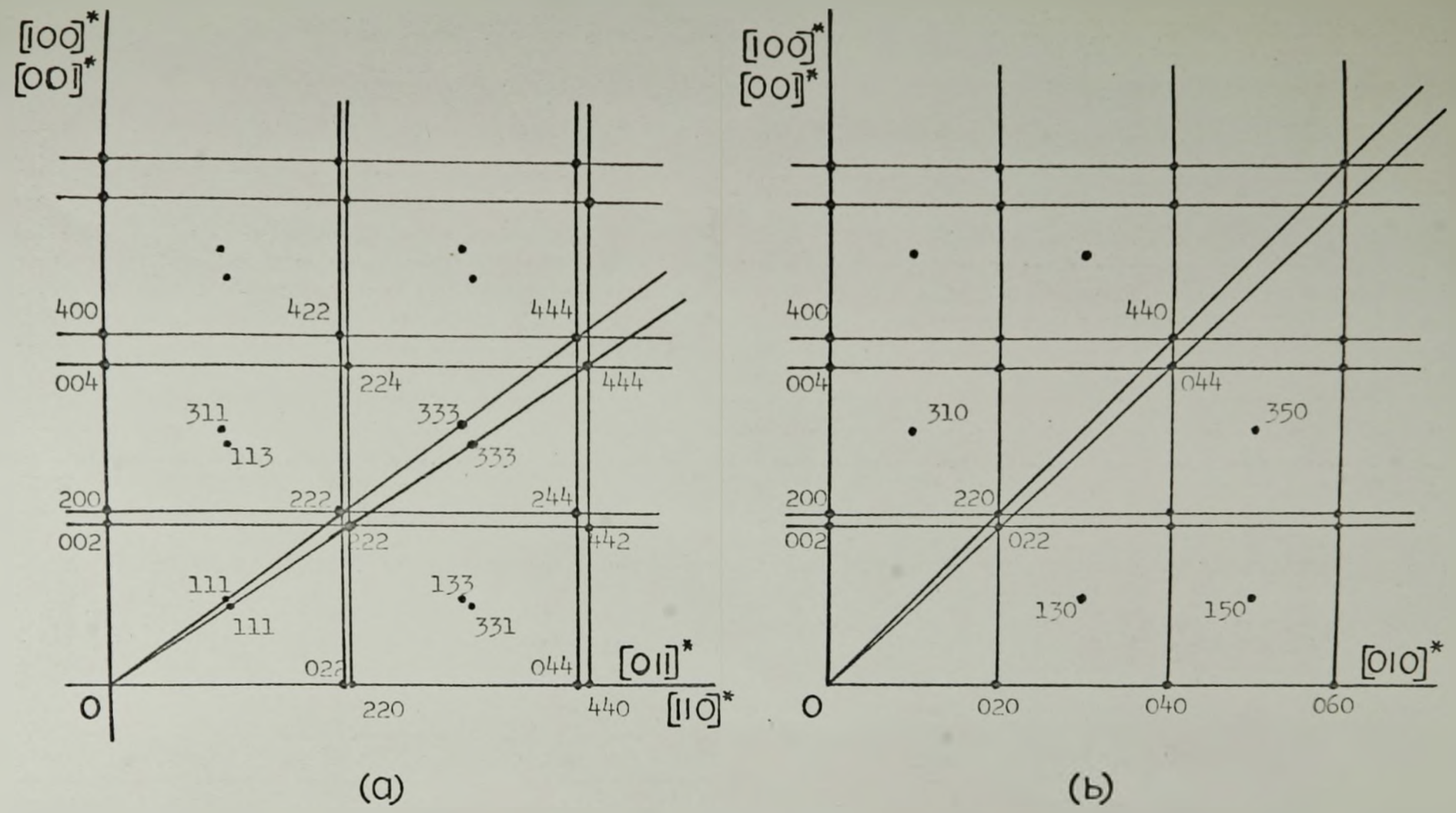

Fig. 9 Twinning in $(NH_4)_2TeBr_6$: Composite reciprocal lattice perpendicular to the C-centered pseudo-cubic tetragonal (a) $[1\bar{1}0]$ and $[0\bar{1}1]$ directions, and (b) $[100]$ and $[001]$ directions.

(N.B. $[001]$ and $[100]$ directions in (b) do not make same angle with normal to the plane of the paper at O).

(400), (600), (800), (1200) and (440) of the room temperature cubic phase. The tetragonal C-centred cell has the dimensions: A=10.606±0.005Å and C=10.765±0.005Å. The ratio of C/A in this case is 1.015; which is similar to 1.010 in K_2SnBr_6 at room temperature (Markstein and Nowotny, 1938). The dimensions of the corresponding primitive cell of the low temperature form of $(NH_4)_2TeBr_6$ are a=7.501±0.005Å and c=10.765±0.005Å.

The following conditions for reflections to occur are noted from the X-ray photographs:

Pseudo cubic cell (C-centred)		Primitive tetragonal cell	
(a-b, b+a, c)		(a, b, c)	
HKO:	H+K = 2n	hkO:	no conditions
HHO:	H = 2n	hOO:	h = 2n
OKL:	K,L = 2n	hhℓ:	ℓ = 2n
HHL:	H+L = 2n	hOℓ:	h+ℓ = 2n

The possible space groups for the primitive cell are $P4/mnc(D_{4h}^6)$ and $P4nc(C_{4v}^6)$. The atoms in the unit cell can be arranged in the following positions:

(I) Space group: $P4nc(C_{4v}^6)$

Te in 2(a): 0,0,z; ½,½,½+z

N in 4(b): 0,½,z; ½,0,z; etc.

Br(1) in 8(a): x,y,z; etc.

Br(2) in 2(a): 0,0,z_1; etc.

Br(3) in 2(a): 0,0,z_2; etc.

(II) Space group: $P4/mnc(D_{4h}^{6})$

Te in 2(a): 0,0,0; $\frac{1}{2},\frac{1}{2},\frac{1}{2}$

H in 4(d): 0,$\frac{1}{2}$,1/4; $\frac{1}{2}$,0,1/4; etc.

Br(1) in 8(h): x,y,0; etc.

Br(2) in 4(e): 0,0,z; etc.

P4/mnc is probably the space group of the low temperature phase since in this space group the $TeBr_6^{2-}$ ion is required to possess a centre of symmetry. In the alternative space group P4nc the bromine atoms are not required to lie centrosymmetrically about the tellurium atom. On the basis of the work performed on this and other related crystals there is no reason for supposing that the $TeBr_6^{2-}$ ion does not have a centre of symmetry.

Table X lists the lattice parameters, space groups and the transition temperatures of $(NH_4)_2TeBr_6$ and K_2SnBr_6 crystals. It is interesting to see that although both the crystals have similar cell constants in the high and low temperature phases and the proposed structures are also very similar, their space groups in the tetragonal phase are different. We can expect that a detailed study of the tetragonal structures of both crystals will throw further light to this point.

The project of collecting single crystal intensity data of $(NH_4)_2TeBr_6$ for complete structure analysis of the low temperature phase was not successful. Several attempts were made to mount crystals

which were found to be untwinned during inspection in the low temperature polarizing microscope; but by the time they were mounted on the goniometer head, these crystals were found to be twinned below the transition temperature.

It is also surprising that the first transition temperature observed in the present study (183°K) is quite different from the value (221°K) reported by Nakamura and his co-workers (1962a). From the observations reported by them it seems that the phase transformation observed in the present work is not different from the one reported. Moreover, no distinct phase transition was observed above 183°K by visual examination or from Weissenberg photographs of the sample. Thus a careful investigation of the phase transition(s) in $(NH_4)_2TeBr_6$ should be undertaken to gather further information for this point.

TABLE X

The Unit Cells and Space Groups of $(NH_4)_2TeBr_6$ and K_2SnBr_6 Crystals

		$(NH_4)_2TeBr_6$	K_2SnBr_6
(1) System:		cubic (298°K)	cubic[a] (403°K)
Space group:		$Fm3m$ (O_h^5)	$Fm3m$ (O_h^5)
Cell constant, a_o:		10.728±0.003A	10.61Å
Phase transition:		tetragonal ⇆ cubic	tetragonal ⇌ cubic
Transition temperature:		183±5°K	400°K[a]
(2) System:			
(i) Pseudocubic cell:		Tetragonal (163°K)	Tetragonal[b] (298°K)
Space group:		$C4/_mcn$ (D_{4h}^6)	$C422_1$ (D_4^2)
Cell constants:	A	10.606 ± 0.005Å	10.51Å
	C	10.765 ± 0.005Å	10.61Å
	C/A	1.015	1.010
(ii) Primitive cell:			
Space group:		$P4/_mnc$ (D_{4h}^6)	$P42_12$ (D_4^2)
Cell constants:	a	7.501 ± 0.005Å	7.43Å
	c	10.765 ± 0.005Å	10.61Å

(a) See Gallioni et al. (1962).

(b) See Markstein and Nowotny (1938).

BIBLIOGRAPHY

Aminoff, B. (1936), Z. Krist 94, 246.

Bagnall, K. W., D'Eye, R. W. M., and Freeman, J. H. (1955) J. Chem. Soc., 3963.

Brown, I. D. (1964) Can. J. Chem. 44, 2758.

Brown, I. D. and Lim, M. M. (1966) Can. J. Chem. (to be published).

Buerger, M. J. (1942) X-ray Crystallography. J. Wiley & Sons, Inc., New York.

Buerger, M. J. (1951) Phase Transformations in Solids, edited by R. Smoluchowski et al., J. Wiley & Sons, Inc., New York p.183.

Buerger, M. J. (1960) Crystal Structure Analysis. J. Wiley & Sons Inc., New York.

Buerger, M. J. (1964) The Precession Method in X-ray Crystallography. J. Wiley & Sons Inc., New York, London, Sydney.

Burbank, R. D. (1952) Rev. Sci. Instr. 23, 321.

Busey, R. H. Dearman, H. H. and Bevan Jr., R. B. (1962) J. Phys. Chem. 66, 82.

Busey, R. H., Bevan Jr., R. B. and Gilbert, R. A. (1965) J. Phys. Chem. 69, 3471.

Busing, W. R. and Levy, H. A. (1964) Acta Cryst. 17, 142.

Cruickshank, D. W. J. (1956a) Acta Cryst. 9, 747.

Cruickshank, D. W. J. (1956b) Acta Cryst. 9, 757.

Engel, G. (1935) Z. Krist. A90, 341.

Ewing, F. J. and Pauling, L. (1928) Z. Krist. 68, 223.

Fernelius, W. C. (1946) Inorganic Syntheses, Vol. II. McGraw Hill Co., Inc., New York p.189.

Galloni, E. E., DeBenyacar, M. R. and DeAbeledo, M.J. (1962) Z. Krist. 117, 407.

Hamilton, W. C. (1955) Acta Cryst. 8, 185.

Hazell, A. C. (1966) Acta Chem. Scand. 20, 165.

Hoard, J. L. and Dickinson, B. N. (1933) Z. Krist. 84, 436.

Ikeda, R., Nakamura, D. and Kubo, M. (1963) Bull. Chem. Soc. Japan 36, 1056.

Ikeda, R., Nakamura, D. and Kubo, M. (1965) J. Phys. Chem. 69, 2101.

International Tables for X-ray Crystallography (1962) Vols. I, II & III, The Kynoch Press, Birmingham, England.

Ito, K., Nakamura, D., Kurita, Y., Ito, K. and Kubo, M. (1961) J. Am. Chem. Soc. 83, 4526.

Ito, K., Nakamura, D., Ito, K. and Kubo, M. (1963) Inorg. Chem. 2, 690.

James, R. W. (1962) The Optical Principles of the Diffraction of X-rays, G. Bell & Sons, London, England.

Lipson, H. and Cochran, W. (1953). The Determination of Crystal Structures, G. Bell & Sons, London, England.

Manojlović, L. M. (1956) Bull. Inst. Nucl. Sci. "Boris Kidrich" Belgrade, 6, 149.

Manojlović, L. M. (1957) Bull. Inst. Nucl. Sci. "Boris Kidrich" Belgrade, 7, 79.

Markstein, G. and Nowotny, H. (1938) Z. Krist. 100, 265.

Morfee, R. G. S., Staveley, L. A. K., Walters, S. T. and Wigley, D. L. (1960) J. Phys. Chem. Solids 13, 132.

Nakamura, D., Kurita, Y., Ito, K. and Kubo, M. (1960) J. Am. Chem. Soc. 82, 5783.

Nakamura, D., Ito, K. and Kubo, M. (1962a) J. Am. Chem. Soc. 84, 163.

Nakamura, D., Ito, K. and Kubo, M. (1962b) Inorg. Chem. 1, 592.

Nakamura, D., Ito, K. and Kubo, M. (1963) Inorg. Chem. 2, 61.

Nakamura, D. and Kubo, M. (1964) J. Phys. Chem. 68, 2986.

Nordman, C. E., Patterson, A. L., Weldon, A. S. and Supper, C. E. (1955) Rev. Sci. Instr. 26, 690.

Pauling, L. (1960) The Nature of the Chemical Bond. Cornell University Press, Ithaca, New York.

Schwochau, K. (1964) Z. Naturforsch, 19a, 1237.

Sieg, L. (1932) Z. anorg. Chem. 207, 93.

Smith, H. G. and Bacon, G. E. (1963) Acta Cryst. 16, A187.

Swanson, H. E., Gilfrich, N. T., Cook, M. I., Stinchfield, R. and Parks, P. C. (1957) Diffraction Powder Patterns Natl. Bur. Std. (U.S.) Circ. No. 539, 8, 5.

Swanson, H. E., Cook, M. I., Isaacs, T. and Evans, E. H. (1960) Diffraction Powder Patterns Natl. Bur. Std. (U.S.) Circ. No. 539, 9, 24.

Templeton, D. H. and Dauben, C. H. (1951) J. Am. Chem. Soc. 73, 4492.

Wahlstrom, E. E. (1960) Optical Crystallography, 3rd Edition J. Wiley & Sons, Inc., New York and London.

Waser, J. (1951) Rev. Sci. Instr. 22, 563, 567.

Werker, W. (1939) Rec. Trav. Chim. 58, 257.

Wiebenga, E. H. and Smits, D. W. (1950) Acta Cryst. 3, 265.